



## Peroxiredoxin AhpC1 protects *Pseudomonas aeruginosa* against the inflammatory oxidative burst and confers virulence

Leonardo Silva Rocha<sup>a,1</sup>, Beatriz Pereira da Silva<sup>b,1</sup>, Thiago M.L. Correia<sup>c</sup>,  
Railmara Pereira da Silva<sup>b</sup>, Diogo de Abreu Meireles<sup>d</sup>, Rafael Pereira<sup>a,c,e</sup>,  
Luis Eduardo Soares Netto<sup>d</sup>, Flavia Carla Meotti<sup>b,\*</sup>, Raphael Ferreira Queiroz<sup>a,f,\*\*</sup>

<sup>a</sup> Programa Multicêntrico de Pós-graduação em Bioquímica e Biologia Molecular, Universidade Estadual do Sudoeste da Bahia, Brazil

<sup>b</sup> Departamento de Bioquímica, Instituto de Química, Universidade de São Paulo, Brazil

<sup>c</sup> Programa Multicêntrico de Pós-graduação Multicêntrico em Ciências Fisiológicas, Instituto Multidisciplinar de Saúde, Universidade Federal da Bahia, Brazil

<sup>d</sup> Departamento de Genética e Biologia Evolutiva, Instituto de Biociências, Universidade de São Paulo, Brazil

<sup>e</sup> Departamento de Ciências Biológicas, Universidade Estadual do Sudoeste da Bahia, Brazil

<sup>f</sup> Departamento de Ciências Naturais, Universidade Estadual do Sudoeste da Bahia, Brazil

### ARTICLE INFO

#### Keywords:

AhpC1  
*P. aeruginosa* (PA14)  
Virulence  
Inflammation  
Oxidants  
Urate hydroperoxide

### ABSTRACT

*Pseudomonas aeruginosa* is an opportunistic bacterium in patients with cystic fibrosis and hospital acquired infections. It presents a plethora of virulence factors and antioxidant enzymes that help to subvert the immune system. In this study, we identified the 2-Cys peroxiredoxin, alkyl-hydroperoxide reductase C1 (AhpC1), as a relevant scavenger of oxidants generated during inflammatory oxidative burst and a mechanism of *P. aeruginosa* (PA14) escaping from killing. Deletion of AhpC1 led to a higher sensitivity to hypochlorous acid (HOCl, IC<sub>50</sub> 3.2 ± 0.3 versus 19.1 ± 0.2 μM), hydrogen peroxide (IC<sub>50</sub> 91.2 ± 0.3 versus 496.5 ± 6.4 μM) and the organic peroxide urate hydroperoxide.  $\Delta$ ahpC1 strain was more sensitive to the killing by isolated neutrophils and less virulent in a mice model of infection. All mice intranasally instilled with  $\Delta$ ahpC1 survived as long as they were monitored (15 days), whereas 100% wild-type and  $\Delta$ ahpC1 complemented with ahpC1 gene ( $\Delta$ ahpC1 attB:ahpC1) died within 3 days. A significantly lower number of colonies was detected in the lung and spleen of  $\Delta$ ahpC1-infected mice. Total leucocytes, neutrophils, myeloperoxidase activity, pro-inflammatory cytokines, nitrite production and lipid peroxidation were much lower in lungs or bronchoalveolar liquid of mice infected with  $\Delta$ ahpC1. Purified AhpC1 neutralized the inflammatory organic peroxide, urate hydroperoxide, at a rate constant of  $2.3 \pm 0.1 \times 10^6 \text{ M}^{-1}\text{s}^{-1}$ , and only the  $\Delta$ ahpC1 strain was sensitive to this oxidant. Incubation of neutrophils with uric acid, the urate hydroperoxide precursor, impaired neutrophil killing of wild-type but improved the killing of  $\Delta$ ahpC1. Hyperuricemic mice presented higher levels of serum cytokines and succumbed much faster to PA14 infection when compared to normouricemic mice. In summary,  $\Delta$ ahpC1 PA14 presented a lower virulence, which was attributed to a poorer ability to neutralize the oxidants generated by inflammatory oxidative burst, leading to a more efficient killing by the host. The enzyme is particularly relevant in detoxifying the newly reported inflammatory organic peroxide, urate hydroperoxide.

### 1. Introduction

The microbial ability to subvert host defense and to develop antibiotic resistance are the main causes of persistent infection and

septicemia. Inhibition of phagocytosis, evasion from phagosome, production of resisting antimicrobial peptides, degradation of neutrophil extracellular traps (NETs) and detoxification of the oxidants produced during inflammatory oxidative burst are well recognized mechanisms

\* Corresponding author. Departamento de Bioquímica, Instituto de Química, Universidade de São Paulo, Brazil Av. Prof Lineu Prestes, 748. Office 1001, CEP: 05508-000, Brazil.

\*\* Corresponding author. Departamento de Ciências Naturais, Universidade Estadual do Sudoeste da Bahia Estrada do Bem Querer, km 04, s/n, CEP: 45031-900, Brazil.

E-mail addresses: [flaviam@usp.br](mailto:flaviam@usp.br) (F.C. Meotti), [rfqueiroz@uesb.edu.br](mailto:rfqueiroz@uesb.edu.br) (R.F. Queiroz).

<sup>1</sup> Both authors equally contribute to this paper.

<https://doi.org/10.1016/j.redox.2021.102075>

Received 17 June 2021; Received in revised form 13 July 2021; Accepted 17 July 2021

Available online 19 July 2021

2213-2317/© 2021 The Authors.

Published by Elsevier B.V. This is an open access article under the CC BY-NC-ND license

(<http://creativecommons.org/licenses/by-nc-nd/4.0/>).

for subverting neutrophil killing [1] [–] [6]. Therefore, bacteria survival will be proportional to the ability of combining the above mechanisms.

These subversion mechanisms are intimately associated with virulence and, in the case of *Pseudomonas aeruginosa*, it is less relevant in healthy individuals though a major cause of acute, hospital-acquired infections, microbial keratitis, as well as chronic lung infections in cystic fibrosis patients [7] [–] [9]. Indeed, *P. aeruginosa* is responsible for ~10% of all hospital-acquired infections worldwide leading to a high mortality rate [10,11]. The bacteria present a plethora of virulence factors including the secretion of cytotoxic and adherence molecules. The effector proteins ExoU, ExoS and ExoT, which are ejected through type III secretion system (T3SS) into the host cell cytosol after phagocytosis, suppress neutrophil response [5,12–14]. ExoS and ExoT suppress immune response mainly through ADP-ribosylation of host proteins. For instance, ExoS ADP-ribosylates Ras, disrupting PI3K signaling, decreasing superoxide production by NADPH oxidase [5,14].

In addition to inhibit superoxide production by the host, *P. aeruginosa* possesses an extraordinary number of antioxidant enzymes. The PA14 strain contains two superoxide dismutase (SodM and SodB); five heme-peroxidases (chloroperoxidase, cytochrome c peroxidase and the catalases, KatA, KatB and KatE); eleven thiol peroxidases (thiol peroxidase - Tpx, cytoplasmic glutathione peroxidase - GPx, periplasmic GPx2 and GPx3, osmotically inducible protein C – OsmC, organic hydroperoxide resistance protein – Ohr, bacterioferritin comigratory protein – Bcp, 1-Cys-peroxiredoxin LsfA and the 2-Cys-peroxiredoxins alkyl hydroperoxide reductases AhpA, AhpB and AhpC) (<https://www.pseudomonas.com>). Despite the vast repertoire presented to counteract oxidants, few studies have focused on the function of these enzymes in *P. aeruginosa* virulence and pathogenicity.

Deletion of KatA decreased PA14 virulence in a model of acute infection in *Drosophila* [15] and peritonitis in mice [16]. Among the thiol peroxidases, only LsfA and Ohr PA14 mutants have been challenged for virulence using models of infection. Knockout of LsfA protein or replacement of the catalytic cysteine by alanine decreased virulence in an acute model of pneumonia in mice [17], whereas knocking out Ohr brought about as much virulence as the wild-type PA14 in *C. elegans* [18]. *In vitro* studies have already demonstrated the role of AhpC, AhpB, Tpx, LsfA and Ohr in the neutralization of hydroperoxides and peroxynitrite [19–23] and a bunch of studies have investigated the role of thiol-peroxidases in the virulence of different microorganisms [19, 24–27].

Considering the unique antioxidant protection system of *P. aeruginosa*, one could assume that inhibition of a single antioxidant protein would not affect bacterial survival or virulence. However, each one of these proteins may have a particular effect against different oxidants and the understanding of this effect would open up a new perspective for antibiotic therapy in such resistant bacterium. In this study, we first evaluated the sensitivity of thiol-peroxidases PA14 mutants to hypochlorous acid (HOCl). We observed a significant sensitivity of the AhpC1 mutant strain ( $\Delta$ ahpC1) and selected it for further virulence studies.  $\Delta$ ahpC1 mutant was more susceptible to the killing by isolated peripheral blood neutrophils. Wild-type PA14 killed 100% mice infected up to 3 days but no death occurred in  $\Delta$ ahpC1 PA14 infected mice up to 15 days. A much lower number of bacteria (CFU) was found in lung and spleen 24 h after mice infection with  $\Delta$ ahpC1 compared to those infected with wild-type PA14. Likewise, a much lower number of total leukocytes and neutrophils was found in bronchoalveolar lavage (BAL) and lung tissue of  $\Delta$ ahpC1 infected mice, with lower IL-1 $\beta$  and TNF- $\alpha$  release. Overall oxidative stress was also lower in  $\Delta$ ahpC1 than wild-type infected mice.

We had previously demonstrated that incubation of neutrophils with uric acid decreased their microbicidal activity against PA14 [28]. Uric acid is the end product of purine metabolism in humans, accumulates in plasma at 50–400  $\mu$ M range, reaching millimolar concentration in hyperuricemia [29]. Uric acid is also abundant in other extracellular fluids and acts as a substrate for the neutrophil enzyme myeloperoxidase to

produce the oxidants urate free radical and urate hydroperoxide. As a consequence, oxidation of uric acid favors a pro-oxidant environment and might have a causal role in vascular diseases [30] [–] [32]. In infection, the oxidation of uric acid by myeloperoxidase and prevention of HOCl formation is a putative cause of the lower ability of neutrophils to kill *P. aeruginosa* [28]. In fact, uric acid oxidation was correlated with a worse prognosis in cystic fibrosis by *P. aeruginosa* [33]. Because urate hydroperoxide is a weaker oxidant than HOCl, the antioxidant arsenal of *P.* may easily neutralize this organic peroxide, explaining why the production of urate hydroperoxide to detriment of HOCl favors bacterial survival. In the present study, we further investigated this effect and found that PA14 lacking AhpC1, but not the wild-type, was significantly sensitive to urate hydroperoxide.  $\Delta$ ahpC1 was also more sensitive to neutrophil killing in presence of uric acid. Hyperuricemic mice were much more sensitive to pulmonary infection by either wild-type or  $\Delta$ ahpC1 strains. These findings open up a new insight on the effect of uric acid in infection conditions since clinical studies have demonstrated a positive correlation between uric acid levels, uric acid oxidation and a worse prognosis in cystic fibrosis and sepsis [33] [–] [37]. The lower virulence of  $\Delta$ ahpC1 strain raises a perspective for adjuvant antibiotic therapy.

## 2. Materials and methods

Sodium chloride, calcium chloride, magnesium chloride, sodium phosphate monobasic, sodium phosphate dibasic, monopotassium phosphate, ammonium sulfate, diethylenetriaminepentaacetic acid (DTPA), uric acid, ammonium acetate, acetonitrile, riboflavin, Chelex-100, Luria-Bertani medium (LB), Müeller Hinton agar (MH), ampicillin, Triton X-100, 3,3',5,5'-tetramethylbenzidine (TMB), H<sub>2</sub>O<sub>2</sub>, 4-aminobenzoic acid hydrazide (ABAH), apocynin, fetal bovine serum albumin, 4,4'-dithiodipyridine, butylated hydroxytoluene (BHT), sodium carboxymethylcellulose medium viscosity, cetyltrimethylammonium bromide (CTAB), dimethyl sulfoxide (DMSO), protease inhibitor cocktail (S8820), EDTA-free protease inhibitor cocktail (11873580001), tryptone, yeast extract, glycerol, anhydrous glucose, tetracycline nalidixic acid, Histopaque-1077 and Histopaque-1119 were purchased from Sigma-Aldrich. Hypochlorous acid was obtained from commercial sodium hypochlorite. Stock solutions of hypochlorous acid were prepared immediately before use, and the concentrations were determined spectrophotometrically in NaOH (0.01 M) ( $\lambda_{290\text{nm}} = 3.5 \times 10^2 \text{ M}^{-1} \text{ cm}^{-1}$ ) [86]. The solutions of H<sub>2</sub>O<sub>2</sub> were prepared before use, and the concentrations were determined spectrophotometrically by reaction with horseradish peroxidase to produce compound I ( $\lambda_{403} = 5.4 \times 10^4 \text{ M}^{-1} \text{ cm}^{-1}$ ) [38]. Minimal medium was made of monobasic sodium phosphate (31 mM), dibasic sodium phosphate (39 mM), ammonium sulfate (18 mM), calcium chloride (100  $\mu$ M), magnesium chloride (2 mM), DTPA (100  $\mu$ M), anhydrous glucose (2%), pH 7.4. PBS-glucose contained dibasic sodium phosphate (10 mM), monopotassium phosphate (1.8 mM), sodium chloride (137 mM), potassium chloride (2.7 mM), anhydrous glucose (1%), pH 7.4. All solutions were prepared in ultrapure water. All buffers were treated with Chelex-100 to remove trace amounts of metal ion contaminants prior to use.

### 2.1. Synthesis and quantification of urate hydroperoxide

The urate hydroperoxide was synthesized as previously described [39,40]. Briefly, 20 mM uric acid (dissolved in 40 mM NaOH), riboflavin (500  $\mu$ M), phosphate buffer (20 mM, pH 6.0) were incubated in a 6-well plate (3.4 cm well diameter) and irradiated at 365 nm for 10 min at 20°C under continuous agitation (UVA light source was equipped with six UVA lamps, 15 mW and 2.2 mW/cm<sup>2</sup>, GE Novatecnica, Campinas-Brazil). The reaction mixture was 4-fold diluted in acetonitrile and the products were separated in a Shimadzu HPLC system (Tokyo, Japan) with two pumps LC-6AD, manual injector CTO-10A, UV

detector UV SPD-20A, system controller CBM-20A connected with a computer with LC solution software. The stationary phase was a preparative TSK-Gel Amide column (10  $\mu\text{m}$ ; 21.5 mm  $\times$  30 cm, TOSOH Bioscience, Tokyo, Japan). The mobile phase consisted of 40% 10 mM ammonium acetate (pH 6.8) and 60% acetonitrile, with a constant flux of 4 mL/min in an isocratic mode for 30 min. Excess of acetonitrile from urate hydroperoxide sample was evaporated with inert gas. To guarantee the maximal removal of the organic solvent, a system equipped with a kitasato flask connected to a vacuum bomb was used. The remaining acetonitrile was quantified by gas chromatography and showed a maximum of 0.07%. Vehicle samples were performed in the presence of mobile phase submitted to acetonitrile evaporation or ammonium acetate. All solutions were stirred with Chelex® 100 Resin (Sigma-Aldrich) for at least 1 h to remove any trace metals. The concentration of urate hydroperoxide was measured by its absorbance at 308 nm ( $\epsilon_{308\text{nm}} = 6540 \text{ M}^{-1} \text{ cm}^{-1}$ ) and compared with the concentration determined by Ferrous Oxidation Xylenol Orange (FOX) as previously described [40].

## 2.2. Bacterial strain and culture

*P. aeruginosa* UCBPP-PA14 (PA14) wild-type (WT) [41] and  $\Delta\text{lsfA}$  [17] and MAR2xT7 mutants,  $\Delta\text{ahpC1}$ ,  $\Delta\text{ahpC2}$ ,  $\Delta\text{ohr}$ ,  $\Delta\text{gpx}$  and  $\Delta\text{ohrR}$  [42] were kindly provided by Prof Dr Regina Baldini, Institute of Chemistry, University of São Paulo, São Paulo, Brazil. Otherwise stated, all strains were grown in Luria-Bertani medium (LB) under shaking at 350 rpm and 37 °C. After ~18 h, cells were diluted in fresh LB to  $\text{OD}_{625\text{nm}} = 0.1$  and incubated until reaching the  $\text{OD}_{625\text{nm}} = 1.2$  ( $1 \times 10^6$  CFU/mL) for late exponential growth phase. Bacterial suspension was then centrifuged at 1700g for 10 min and suspended in an equal volume of either minimal medium or PBS-glucose according to the experiment.

For a single copy *ahpC1* complementation, the fragment of 1172 pb corresponding to *ahpC1* with its native promoter was PCR amplified from genomic DNA of PA14 strain using primers *ahpC1*-compl\_F-ATGCGGATCCTACCTGTCGCTGGCCTACAC and *ahpC1*-compl\_R-ATGCAAGCTTGAAATTCGGGCAAACGTATC, cloned into BamHI/HindII restrictions sites of integrative mini-CTX2 vector and sequenced, originating mini-CTX2-*pahpC* construct. Integration at the *attB* site of *P. aeruginosa* PA14 *ahpC*:MAR2xT7 strain was done by conjugation with *E.coli* S17.1  $\lambda\text{pir}$  donor strain harboring mini-CTX2-*pahpC* construct. *P. aeruginosa* PA14 *ahpC*:MAR2xT7 transconjugants were selected by plating the bacterial conjugation in LB supplemented with tetracycline (100  $\mu\text{g}/\text{mL}$ ) and nalidixic acid (20  $\mu\text{g}/\text{mL}$ ). The integration was confirmed by PCR (*ahpC*\_conf\_L - CATCTGGTGCTGGTCCT and *ahpC*\_conf\_R - AAATTCGGGCAAACGTATC), originating strain PA14 *ahpC*:MAR2xT7 *attB*:ctx2-*pahpC* [43].

## 2.3. Bactericidal activity of oxidants

PA14 strains ( $1 \times 10^6$  CFU/mL) were incubated with HOCl (5–50  $\mu\text{M}$ ),  $\text{H}_2\text{O}_2$  (0.01–4 mM) or urate hydroperoxide (5–100  $\mu\text{M}$ ) in minimal medium at 37 °C. After 30 min, bacterial suspension was 200-fold diluted in LB, and 10  $\mu\text{L}$  were plated onto Muller Hinton (MH) agar plates. Plates were maintained at 30 °C for 18–20 h and bactericidal activity was estimated by counting CFU [28]. The  $\text{IC}_{50}$  values were calculated using GraphPad Prism. The dose-response curve using the logarithmic concentrations of the oxidants was fitted to a sigmoid.

## 2.4. Purification of human neutrophils

Human neutrophils were isolated from fresh peripheral blood of healthy donors (25  $\pm$  5 years old) by gradient centrifugation [44] with minor modifications. Blood was harvested in a sterile sodium heparin vacutainer, and homogenized by slow inversion. Next, 3 mL of Histopaque 1119 was placed in a 15 mL conical tube, carefully overlaid with 2 mL of Histopaque 1077, and 4 mL of blood. After 30 min centrifugation

at 700g, room temperature, neutrophil layer was obtained from the interface between both gradients. Erythrocytes were discarded by hypotonic hemolysis in ice-cold ultrapure water with 10 min centrifugation at 300g. The resulting pellet was suspended in 2 mL PBS-glucose, cells were counted in a Neubauer chamber (Sigma-Aldrich, MA, EUA) using trypan blue (0.2%) exclusion method [45]. The protocol was approved by Human Research Ethics Committee from Universidade Estadual do Sudoeste da Bahia (#46135315.4.0000.0055).

## 2.5. Bactericidal activity of neutrophils

WT,  $\Delta\text{ahpC1}$  or  $\Delta\text{ahpC2}$  complemented with *ahpC1* gene ( $1 \times 10^7$  CFU/mL) were first opsonized in PBS-glucose containing inactivated autologous human serum (10%) for 20 min at 37 °C. Human neutrophils ( $1 \times 10^6$  cells/mL) were incubated with each strain (MOI = 1:10) in presence or absence of uric acid (200 and 400  $\mu\text{M}$ ), 4-aminobenzoic acid hydrazide (50  $\mu\text{M}$ , ABAH, a myeloperoxidase inhibitor), or apocynin (1 mM, APO, a NADPH oxidase inhibitor). After 1 h, Triton X-100 (10%) was added for neutrophil lysis. Cell lysate was serially diluted  $10^4$ -fold in PBS-glucose, and 10  $\mu\text{L}$  were spread onto MH agar plates for 18–20 h at 30 °C for CFU counting [28,46].

## 2.6. Expression and purification of AhpC

The *ahpC* gene was PCR-amplified from the 07B05 cosmid used in the *Xylella fastidiosa* Genome Project. The PCR product was cloned into the NdeI and BamHI restrictions sites of pET15b vector. Subsequently, *E. coli* BL21(DE3) strain was transformed by heat shock method to allow expression of pET15b-*ahpC* and cultured overnight at 37 °C in 50 mL of LB-ampicillin, transferred to 1 L of fresh LB-ampicillin and incubated until reaching  $\text{OD}_{600\text{nm}} = 0.6$ . Isopropyl-beta-D-thiogalactopyranoside (IPTG) was added to a final concentration of 1 mM. After 3 h of incubation, cells were harvested by centrifugation. The pellet was washed and suspended in 20 mL lysis buffer (Tris-HCl 50 mM, NaCl 100 mM, lysozyme 1 mg/mL, glycerol 10%, 1 tablet EDTA-free protease inhibitor cocktail, pH 7.4). After incubation on ice for 10 min, cells were submitted to sonication at 30% amplitude for 5 min on ice, 20 s on and 40 s off. The suspension was centrifuged at 31,500g for 30 min at 4 °C and the supernatant was loaded onto a nickel affinity column (HiTrap™, GE Healthcare). The conditions of protein purification were optimized using the manual gradient of imidazole as described by the manufacturer. SDS-PAGE was used to check the purification quality, and all fractions containing bands with MW ~23 kDa were combined, concentrated through Amicon Ultra 10 kDa ultrafiltration (Millipore Corporate, Germany). Protein concentration was measured spectrophotometrically ( $\epsilon_{280\text{nm}} = 27,055 \text{ M}^{-1} \text{ cm}^{-1}$ ) [47].

Basic Local Alignment Search Tool (BLAST) was used to compare the sequence of AhpC1 and AhpC2 from PA14 (A0A072ZH89 and A0A071KYB2, respectively) with AhpC from *Xylella fastidiosa* (Q87DE0). AhpC1 from PA14 and AhpC from *X. fastidiosa* share 61% identity, 78% homology, with both peroxidic Cys47 and resolving Cys165 conserved among the two species (Supplem Fig. 1).

## 2.7. Pre-reduction of AhpC and quantification of protein thiols

Immediately before the experiments, AhpC was reduced with DTT (in a 5-fold molar excess of thiols) for 2 h at 37 °C under an argon atmosphere. The remaining DTT was removed by filtration through an Amicon Ultra-15 10K filter (Millipore) against 50 mM phosphate buffer pH 7.4 containing DTPA (100  $\mu\text{M}$ ). For all experiments related to AhpC, phosphate buffer was previously treated with bovine catalase (10  $\mu\text{g}/\text{mL}$ ) before filtration through an Amicon Ultra-15 10K filter (Millipore). Protein thiols were determined by incubating 5  $\mu\text{L}$  samples with 95  $\mu\text{L}$  0.25 mM 4,4'-dithiodipyridine, 1% SDS for 10 min in the dark and read at 324 nm ( $\epsilon_{324\text{nm}} = 21,400 \text{ M}^{-1} \text{ cm}^{-1}$ ).

## 2.8. Stopped-flow experiment

AhpC oxidation to sulfenic acid was followed by monitoring intrinsic fluorescence decay [48] [–] [51]. Pre-reduced AhpC (0.5  $\mu\text{M}$  or 1  $\mu\text{M}$  with  $\sim 1.5$   $\mu\text{mol SH}/\mu\text{mol protein}$ ) was mixed with increasing concentrations of  $\text{H}_2\text{O}_2$  or urate hydroperoxide in a stopped-flow instrument (Applied Photophysics SX20MV, Leatherhead, United Kingdom), excitation  $\lambda_{280\text{nm}}$ , emission above  $\lambda_{340\text{nm}}$ . The reactions were performed at 25°C in 50 mM sodium phosphate buffer pH 7.4 containing diethylenetriaminepenta-acetic acid (100  $\mu\text{M}$ , DTPA). Buffer solutions were pre-treated with 10  $\mu\text{g}/\text{mL}$  catalase to remove any trace of  $\text{H}_2\text{O}_2$  [52]. After that, catalase was removed through filtration using an Amicon Ultra-15 10K filter (Millipore). A slight excess of  $\text{H}_2\text{O}_2$  was used that approximates pseudo-first order condition. A proper 10-fold excess of  $\text{H}_2\text{O}_2$  is not possible to monitor because the reaction occurs before the dead time of the equipment ( $\sim 2$  ms). A much larger excess of urate hydroperoxide was used to allow pseudo-first order conditions. Observed rate constants ( $k_{\text{obs}}$ ) for fluorescence decrease were determined by fitting data to single exponential equations. The fittings were set from 2 ms. The values of  $k_{\text{obs}}$  obtained from the decreasing fluorescence were plotted against  $\text{H}_2\text{O}_2$  or urate hydroperoxide concentrations and the corresponding second order rate constants were determined from the slope of these linear fittings.

## 2.9. Animals

Male C57BL/6 mice (8 weeks old,  $25 \pm 1$  g) were obtained from Anilab (Paulinia, São Paulo, Brazil). Mice were maintained under 12/12 h light/dark cycle with free access to water and commercial standard feed (Pragsoluções, São Paulo) under pathogen-free conditions and controlled temperature ( $23 \pm 3$  °C). The procedures were approved by the Ethics Committee for experiments with animals from the Universidade Estadual do Sudoeste da Bahia (#171/2018).

## 2.10. Intranasal infection, mice survival and tissue collection

WT,  $\Delta\text{ahpC1}$  and  $\Delta\text{ahpC1}$  complemented with  $\text{ahpC1}$  were grown as described above. After overnight incubation, bacteria were diluted into fresh LB to  $\text{OD}_{625\text{nm}}=0.6$ , centrifuged at 4500g for 8 min, and the pellet was suspended at  $6.7 \times 10^7$  CFU/mL in sterile saline. Mice ( $n = 8/\text{group}$ ) were first anesthetized with ketamine (50 mg/kg) and xylazine (16 mg/kg), before nasal instillation of 30  $\mu\text{L}$  bacterial suspension ( $2 \times 10^6$ , each strain) or sterile saline [53]. Mice were observed twice daily for survival up to 15 days. To avoid excessive suffering, mice were systematically euthanized by cervical dislocation when they were found in a moribund state with at least four of the following distress criteria: inability to maintain upright, associated or not with labored breathing and cyanosis, anorexia and weight loss ( $>20\%$ ), hunching, prostration, impaired motility, ruffled haircoat and dehydration [54]. Mice were intranasally inoculated with WT,  $\Delta\text{ahpC1}$ ,  $\Delta\text{ahpC1attB}::\text{ahpC1}$  or sterile saline, as described above. Twenty-four hours later, they were anesthetized by i.p. administration of a mix of ketamine (50 mg/kg) and xylazine (16 mg/kg) for bronchoalveolar lavage harvesting, followed by cervical dislocation [55] for tissue collection as described below.

## 2.11. Bronchoalveolar lavage

Immediately after anesthesia, mice underwent tracheostomy for tracheal cannulation with infusion catheter (G22) and the lungs were washed three times with 0.5 mL PBS glucose for BAL collection. Cells were diluted in Turk's solution (NewProv) and total leukocyte count was performed in a Neubauer chamber. Then, 50  $\mu\text{L}$  of BAL were centrifuged at 4,500g for 7 min onto a glass lamina and stained with Rapid Panotic Kit (NewProv). A total of 100 cells per lamina were assessed by double-blind counting, following standard morphological criteria [56]. The remaining BAL was centrifuged at 1500g for 10 min at 4 °C, and the

supernatant was kept at  $-80$  °C until nitrite determination.

## 2.12. Tissue harvesting

The euthanized animals underwent mid-thoracotomy for lung harvesting after BAL harvesting. The right lung was first divided longitudinally in two: one half was used for CFU counting; the other half was snap-frozen in liquid nitrogen and stored at  $-80$  °C for biochemical analysis. One half of the left lung was immersed in Methacarn fixative solution (60% methanol, 30% chloroform and 10% acetic acid) for 24 h, followed by ethanol (70%) washing for histological analyses and the other half was snap-frozen in liquid nitrogen and stored at  $-80$  °C for cytokines levels assessment.

## 2.13. Survival curve in hyperuricemic mice

Mice were intraperitoneally injected with potassium oxonate (300 mg/kg) to induce hyperuricemia [57]. Potassium oxonate was freshly dissolved in 0.5% sodium carboxymethylcellulose and daily injected for 6 days. After 22 h from the first potassium oxonate administration, mice were randomly divided into three groups that were nasally instilled with sterile saline (sham,  $n = 6$ ), WT ( $n = 7$ ) or  $\Delta\text{ahpC1}$  ( $n = 7$ ) PA14 as described above. Mice were observed twice daily for survival up to 5 days after bacteria instillation and excessive suffering was avoided as described above and described elsewhere [54]. Concomitantly, a separate group of mice ( $n = 6$ ) received only 0.5% sodium carboxymethylcellulose for 6 days as vehicle control. On the 7th day following potassium oxonate or vehicle treatment, the sterile saline instilled mice, the only survival ones, were anesthetized with xylazine/ketamine as above and decapitated for blood harvesting to assess serum cytokines and uric acid. Blood samples were centrifuged at 1,500g for 10 min at room temperature and then stored at  $-80$  °C. Serum uric acid was assessed by a mono-reagent kit (Bioclin, Brazil) following the manufacturer's specification.

## 2.14. Cytokine levels

IL-1 $\beta$  and TNF- $\alpha$  from serum or lung homogenate were determined using the enzyme-linked immunosorbent assay (ELISA) kits (DY401-05 and DY410-05, respectively) according to the manufacturer's instructions (R&D System), except by incubation of the samples with the pre-coated microplates for 16 h at 4–8 °C. Lung homogenate was diluted two-fold in diluent reagent before running the ELISA. The cytokine concentrations were expressed as pg/mL or pg/mg of protein for serum or lung homogenate, respectively.

## 2.15. Determination of nitrite in BAL

Nitrite was measured by the Griess method [58]. BAL supernatant (50  $\mu\text{L}$ ) was incubated with 50  $\mu\text{L}$  naphthylethylenediamine solution (0.1%) and 50  $\mu\text{L}$  sulfanilamide 209 solution (1%) for 10 min at 25°C. Sample absorbance was determined at 540 nm and interpolated against a standard curve of nitrite (1.65–100  $\mu\text{M}$ ).

## 2.16. Tissue CFU counting

Immediately after euthanasia, organs (100 mg/mL) were homogenized in cold PBS buffer using a TissueRuptor system (Qiagen, USA) [59]. Ten microliters homogenate were spread onto MH agar plates and incubated for 18–20 h at 30 °C [17]. The bacterial colonies were counted and the CFU was expressed by g of wet tissue.

## 2.17. Histological analyses

Fixed and dehydrated lungs were soaked in paraffin, cut longitudinally in 4  $\mu\text{m}$ -thick microtome sections (Leica RM2125RTS, CN) and

stained with hematoxylin and eosin (H&E). Neutrophils were counted in 30 random fields using a digital camera (Kontron Electronic KS-300, Eching, GE) coupled to a light microscope (BX51, Olympus, JP) under 400 × magnification. Neutrophil numbers per field were quantified using Image J 1.44P software (National Institutes of Health, US).

### 2.18. Peroxidase activity

Lung tissue (100 mg/mL) was homogenized in potassium phosphate buffer (50 mM), pH 6.0 and centrifuged at 4°C, 10,000g for 10 min. Cetyltrimethylammonium bromide (CTAB, 0.5%) was added to the supernatant to prevent MPO adhesion to tube walls. The homogenate (10 µL) was mixed with 110 µL working solution containing 3,3', 5,5'-tetramethylbenzidine (TMB, 2.9 mM dissolved in 14% dimethylsulfoxide and 86% 150 mM sodium phosphate buffer, pH 5.4). Reaction was initiated by adding 80 µL H<sub>2</sub>O<sub>2</sub> (0.75 mM). TMB oxidation was monitored every 30 s at 450 nm (Thermoplate, Tp-reader, US) for 5 min at 25°C ( $\epsilon_{450\text{nm}} = 5.9 \times 10^4 \text{ M}^{-1} \text{ cm}^{-1}$ ). The MPO inhibitor, 4-Aminobenzoic acid hydrazide (ABAH, 50 µM) was added to a lung sample from WT-infected mice to evaluate MPO contribution to the peroxidase activity. Results were expressed as specific activity (U/mg protein), where one unit of peroxidase activity was defined as the amount of enzyme that produced 1 µmol of oxidized TMB per min at 25 °C [60].

### 2.19. Quantification of thiobarbituric acid reactive products

Lipid peroxidation was estimated by thiobarbituric acid reactive substances (TBARS) assay [61]. Right lung tissue (100 mg/mL) was homogenized in 50 mM Tris-HCl buffer, pH 8.0, containing butylated hydroxytoluene (BHT, 0.02%) to prevent spurious oxidation. The homogenate was centrifuged at 1,600g for 10 min at 4°C. The supernatant was then diluted (1:2) in 100 µL TrisHCl and incubated with 100 µL trichloroacetic acid (10%) and 800 µL thiobarbituric acid (0.53%, dissolved in 20% acetic acid) for 1 h at 95°C. After cooling on ice for 10 min, samples were again centrifuged at 1,600g for 10 min at 4°C, and absorbance was recorded at 535 nm. TBARS levels were estimated by interpolating sample absorbance on a standard curve of malondialdehyde (Cayman Chemical, US) (0–50 µM), normalized by protein concentration and expressed as µmol of MDA/g of protein.

### 2.20. Determination of total protein concentration

Total protein concentration in lung homogenates was determined by Bradford colorimetric assay at 595 nm [62] employing serum bovine albumin (Sigma-Aldrich, US) (0–1.4 mg/mL) as standard.

### 2.21. Statistical analyses

All analyses were performed in GraphPad Prism (v. 5.0). Data are expressed as mean ± standard error of the mean. Statistical significance was calculated with one-way ANOVA and Newman-Keuls as post-test, when appropriate. Kaplan-Meier survival curves were plotted and the significance was calculated using the log-rank test. Differences were considered significant when  $p < 0.05$ . Data reproducibility is demonstrated by the number of independent experiments in each figure legend.

## 3. Results

Initially, we tested the sensitivity of different PA14 mutants to HOCl and among all the strains analyzed  $\Delta\text{ahpC1}$  was the most sensitive (Table 1). A dose-response curve for HOCl inhibiting wild-type and  $\Delta\text{ahpC1}$  survival is demonstrated in Fig. 1A. As depicted in Fig. 1B–C,  $\Delta\text{ahpC1}$  was also more sensitive to H<sub>2</sub>O<sub>2</sub> (IC<sub>50</sub> 91.2 ± 0.3 µM) than wild-type (IC<sub>50</sub> 496.5 ± 6.4 µM). By reinserting the *ahpC1* gene to  $\Delta\text{ahpC1}$ , the bacterial resistance was restored to wild type level, the IC<sub>50</sub> for H<sub>2</sub>O<sub>2</sub> was 660.3 ± 2.9 µM for this strain (Fig. 1D).

**Table 1**

Inhibition of HOCl on bacterial growth.

Strain	IC <sub>50</sub> HOCl (µM)
WT	19.1 ± 0.2
$\Delta\text{ahpC1}$	3.2 ± 0.3
$\Delta\text{ahpC2}$	10.0 ± 0.1
$\Delta\text{ohr}$	13.7 ± 0.4
$\Delta\text{lsfA}$	10.4 ± 0.4
$\Delta\text{gpx}$	6.7 ± 0.2

Data are expressed as mean ± SEM of two independent experiments performed in triplicate.

We then compared the sensitivity of wild-type and  $\Delta\text{ahpC1}$  strains to neutrophils,  $\Delta\text{ahpC1}$  was slightly but significantly more sensitive to neutrophil killing than wild-type. The inhibition of NADPH oxidase by apocynin or myeloperoxidase by ABAH significantly prevented the killing activity of neutrophils (Fig. 2A). The complementation of the  $\Delta\text{ahpC1}$  mutant with *ahpC1* again reverted the resistance to the wild-type level (Fig. 2B).

When wild-type and  $\Delta\text{ahpC1}$  mutant strains were instilled via intranasal into mice, an enormous difference in the virulence between both strains was observed. Whereas wild-type PA14 killed 100% mice infected up to 3 days, no death occurred in  $\Delta\text{ahpC1}$  PA14 infected mice up to 15 days. The reinsertion of *ahpC1* into the  $\Delta\text{ahpC1}$  PA14 ( $\Delta\text{ahpC1}$  *attB:ahpC1*) completely restored the virulence, as this strain also killed 100% mice up to 3 days of infection (Fig. 3A). In accordance with a lower virulence of  $\Delta\text{ahpC1}$  PA14, a much lower number of bacteria (CFU) was found in lung and spleen 24 h after infection with  $\Delta\text{ahpC1}$  compared to wild-type PA14 (Fig. 3B).

As a consequence, a much lower number of total leukocytes and neutrophils was found in bronchoalveolar lavage (BAL) of  $\Delta\text{ahpC1}$  infected mice compared to wild-type (Fig. 4). Total neutrophil was also lower in the lung parenchyma of  $\Delta\text{ahpC1}$  than wild-type infected mice, as confirmed by quantitative hematoxylin-eosin histological counting and peroxidase activity (Fig. 5A and B). The peroxidase activity was likely due to MPO because ABAH completely abrogated the TMB (Fig. 5B). Pro-inflammatory cytokines IL-1β and TNF-α were significantly higher in lungs of wild-type than  $\Delta\text{ahpC1}$  infected mice (Fig. 5C). Overall oxidative stress was also lower in  $\Delta\text{ahpC1}$  than wild-type infected mice, as observed by lipoperoxidation in lung (Fig. 6A) and nitrite production (Fig. 6B). Together, these results suggested that the absence of AhpC1 in PA14 increases the susceptibility of the bacteria to the killing by the immune system, shortening the bacteria clearance from lung and decreasing tissue inflammation. The lower virulence of  $\Delta\text{ahpC1}$  strains is likely due to a lower ability to neutralize the oxidants generated during the inflammatory oxidative burst leading to a more efficient killing.

Previously, we had demonstrated that PA14 was more resistant to the killing by neutrophils in presence of uric acid. We found that the oxidation of uric acid by the neutrophil heme-peroxidase, myeloperoxidase, decreased HOCl formation and, consequently, the microbicidal activity of these cells [28]. Because the oxidation of uric acid by myeloperoxidase generates the oxidants urate free radical and urate hydroperoxide, we asked whether AhpC1 could neutralize urate hydroperoxide and contribute to bacteria resistance against this oxidant. Here, we reproduced those previous findings as physiological concentrations of uric acid (200 and 400 µM) significantly protected PA14 from killing by neutrophils (Fig. 7, white bars). Interestingly, uric acid had the opposite effect to  $\Delta\text{ahpC1}$  mutant since it increased even more the killing capability of neutrophils against this strain (Fig. 7, grey bars). This result suggests that AhpC1 is indeed important for protecting bacteria from alternative oxidants, such as the organic peroxide, urate hydroperoxide. Because urate hydroperoxide is a weaker oxidant than HOCl, it is not as efficient as the latter to kill PA14. However, in the absence of AhpC1, which likely neutralizes urate hydroperoxide, it becomes an efficient microbicide.

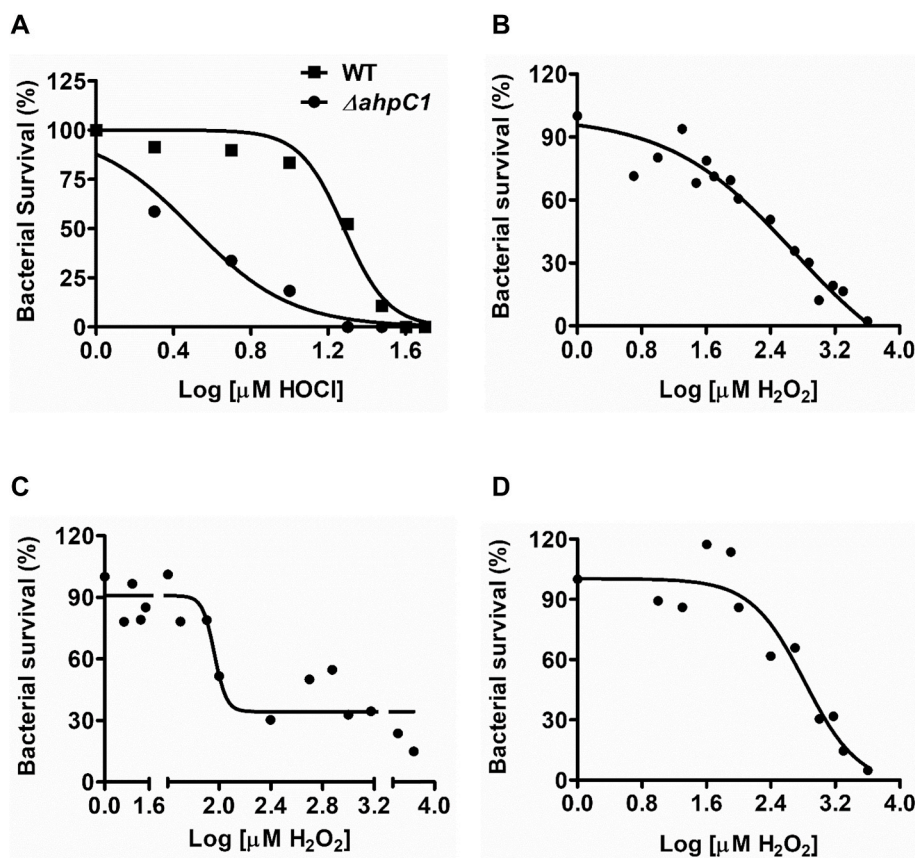


**Fig. 1.** Microbicidal activity of oxidants to PA14. (A) Microbicidal activity of HOCl to wild-type (WT) and  $\Delta ahpC1$  strains. Microbicidal activity of  $H_2O_2$  to (B) wild-type, (C)  $\Delta ahpC1$  and (D)  $\Delta ahpC1$  expressing *ahpC1* by gene reinsertion ( $\Delta ahpC1 attB::ahpC1$ ). Bacteria ( $1 \times 10^6$  CFU/mL) were incubated with HOCl or  $H_2O_2$  at 37°C in minimal medium for 30 min, then diluted 200-fold in LB medium and spread onto MH agar for 18–20 h at 30°C. Data are representative of 3–4 independent experiments. A logarithmic dose-response curve was fitted to a sigmoid and  $IC_{50}$  values were calculated using GraphPad Prism.

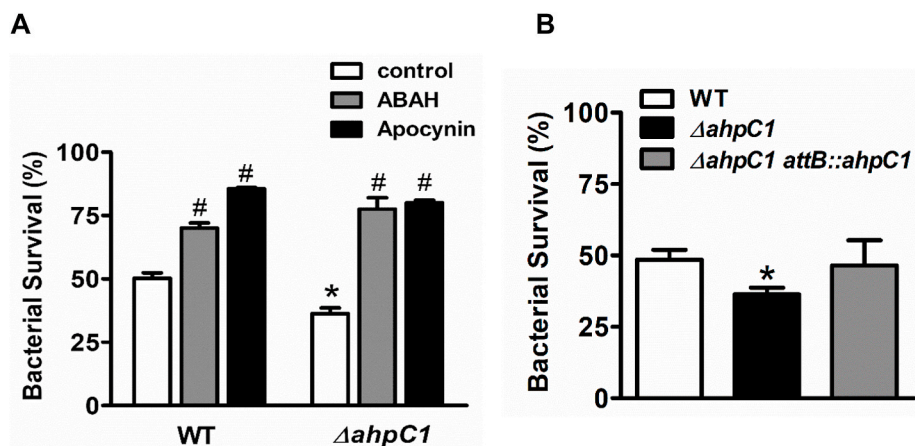


**Fig. 2.** Bacterial survival after incubation with neutrophils. (A) Opsonized wild-type or  $\Delta ahpC1$  ( $1 \times 10^7$  CFU/mL) were incubated with neutrophils ( $1 \times 10^6$  cells/mL) for 1 h, with or without ABAH (50  $\mu$ M) or apocynin (1 mM). (B) Opsonized wild-type,  $\Delta ahpC1$  or  $\Delta ahpC1 attB::ahpC1$  ( $1 \times 10^7$  CFU/mL) were incubated with neutrophils ( $1 \times 10^6$  cells/mL) for 1 h. Neutrophils were lysed, samples were diluted 10,000-fold in PBS-glucose. Ten microliters were spread onto MH agar plates, grown for 18–20 h at 30°C and then submitted to CFU counting. Data are plotted as mean  $\pm$  SEM (n = 2 to 3 per group). Statistical analyses were performed by one-way ANOVA analysis of variance followed by Neuman-kels. \*p < 0.05 indicates a significant difference from wild-type (WT) and #p < 0.05 indicates a significant difference from wild-type or  $\Delta ahpC1$  control groups.

To look further in this direction, we incubated purified urate hydroperoxide with wild-type,  $\Delta ahpC1$  and  $\Delta ahpC1 attB::ahpC1$ . Urate hydroperoxide was unable to kill wild-type and the complemented  $\Delta ahpC1 attB::ahpC1$  (Fig. 7B and D), but it reduced  $\Delta ahpC1$  strain counting at low concentrations (Fig. 7C).

To prove that AhpC1 can indeed neutralize urate hydroperoxide, we calculated the rate constant for the reduction of urate hydroperoxide by the recombinant AhpC from *Xylella fastidiosa*. AhpC1 from PA14 and AhpC from *X. fastidiosa* share 61% identity, 78% homology, with both peroxidatic Cys47 and resolving Cys165 conserved among the two species (Supplem Fig. 1). By mixing AhpC with crescent concentrations of urate hydroperoxide or  $H_2O_2$  a fast drop in the intrinsic fluorescence was observed, which is consistent with the oxidation of the enzyme [48] [–] [50] (Fig. 8A and C). The plot of  $k_{obs}$  versus urate hydroperoxide

(Fig. 8B) or  $H_2O_2$  (Fig. 8D) concentrations gave a second-order rate constant of  $2.3 \pm 0.09 \times 10^6$  and  $1.5 \pm 0.07 \times 10^8$   $M^{-1}s^{-1}$ , respectively. These values are much in agreement with those calculated by the reaction of urate hydroperoxide with human 2-Cys Prx2 [49] and by  $H_2O_2$  with human 2-Cys Prx2 and AhpC from *Salmonella typhimurium* [50, 63–65]. AhpC also seems to react faster with HOCl, however, we could not determine the rate constant by fluorescence since HOCl also oxidizes the tryptophan residues altering protein fluorescence (data not shown).

We next evaluate the effect of uric acid upon wild-type and  $\Delta ahpC1$  PA14 infection *in vivo* using a pharmacological model of mouse hyperuricemia. In this model, mice were daily treated with potassium oxonate, an inhibitor of uricase, suspended in carboxymethylcellulose for slow release. A single injection of oxonate is enough to maintain hyperuricemia for at least 24 h [57]. Indeed, the concentration of uric acid

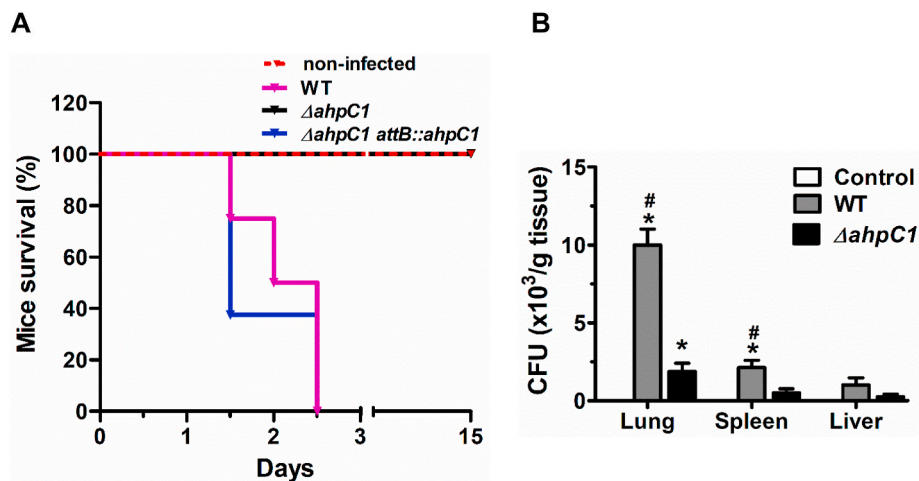


**Fig. 3.** (A) C57BL/6 mice survival after intranasally instillation of sterile saline (non-infected), WT,  $\Delta ahpC1$  or  $\Delta ahpC1 attB::ahpC1$  strains ( $2 \times 10^6$  CFU/mL). Mice were observed twice a day for survival or any other distress up to 15 days. (B) C57BL/6 mice were intranasally instilled with sterile saline (Control), WT or  $\Delta ahpC1$  strains ( $2 \times 10^6$  CFU/mL) and euthanized after 24 h. Tissues were harvested, macerated in PBS-glucose and the supernatant was diluted and spread onto MH agar plates. CFU was counted after growth for 18–20 h at 30°C. Each bar represents mean  $\pm$  SEM of 8 mice in the infected group and 3 mice in the control group. Statistical analyses were performed by one-way ANOVA analysis of variance followed by Newman-Keuls. \* $p < 0.05$  indicates a significant difference from control (non-infected) and # $p < 0.05$  indicates a significant difference to  $\Delta ahpC1$  group.

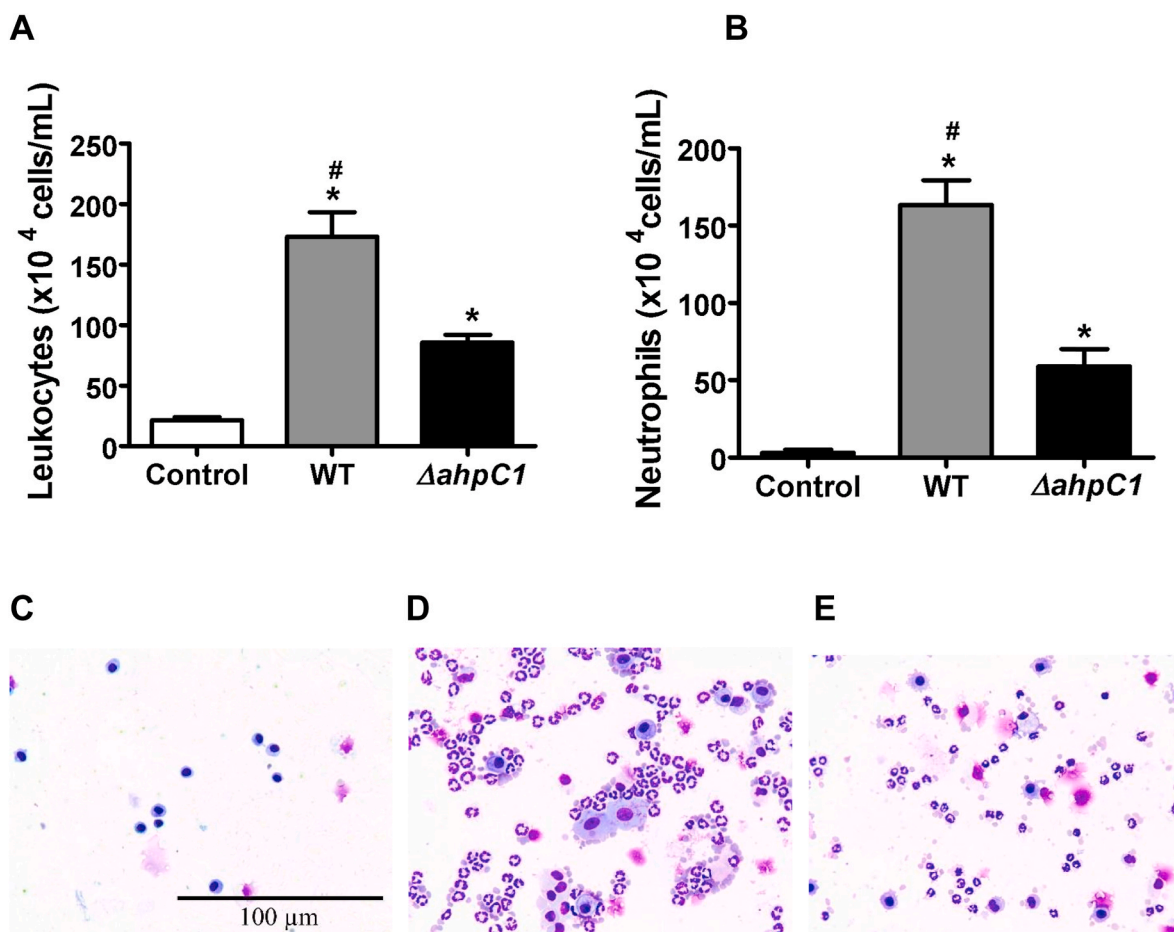


**Fig. 4.** Total leukocytes (A) and neutrophils (B) in broncho-alveolar lavage (BAL) after intranasal infection with wild-type or  $\Delta ahpC1$  ( $2 \times 10^6$  CFU/mL) strains. After 24 h of bacterial nasal instillation, BAL was collected and the cells were diluted in Turk's liquid and counted in a Neubauer chamber. Differential leukocyte count was performed after centrifugation of 50  $\mu$ L of sample, staining with rapid Panotic method and counting of a total of 100 cells. Representative photomicrographs of the cell count in the BAL of mice C57BL/6 control (C), inoculated with WT (D) or  $\Delta ahpC1$  strains (E). Data are expressed as mean  $\pm$  SEM of 8 animals for the infected groups and 3 animals for the control group. Statistical analyses were performed by one-way ANOVA analysis of variance followed by Newman-Keuls. \* $p < 0.05$  indicates a significant difference from control (non-infected) and # $p < 0.05$  indicates a significant difference from the  $\Delta ahpC1$  group.

was nearly 3-fold higher in mice treated with oxonate ( $5.25 \pm 0.12$  mg/dL) versus those treated with vehicle ( $1.73 \pm 0.01$  mg/dL) on the 7th day following oxonate injection (Fig. 9B). Hyperuricemia highly enhanced infection-induced mortality. All mice died 24 h after intranasal instillation of wild-type PA14 (Fig. 9A), twice faster than the

mortality caused by this same strain in non-hyperuricemic mice (Fig. 3A). In addition, nasal instillation with  $\Delta ahpC1$  PA14 killed nearly 40% mice up to 48 h and 100% within 72 h (Fig. 9A), being extensively more aggressive than in non-hyperuricemic mice, which had 100% survival within the 15 days of evaluation (Fig. 3A). No death occurred in

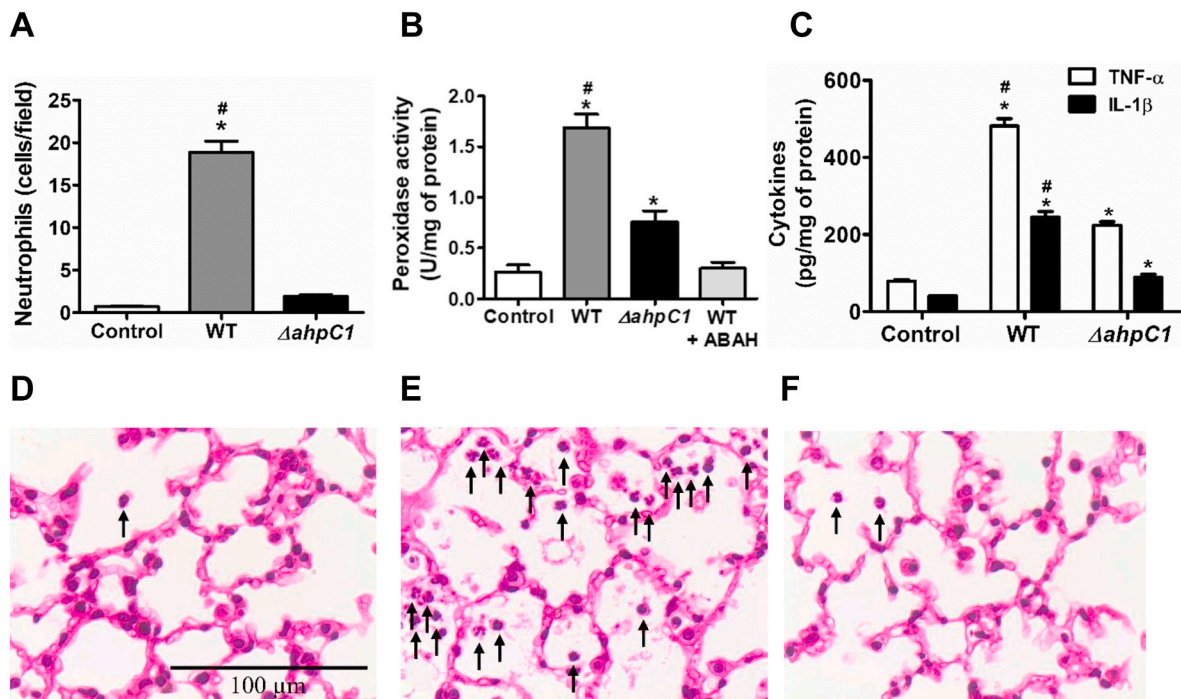


**Fig. 5.** Total neutrophils (A) peroxidase activity (B) and cytokines (C) in lung tissues after 24 h of infection. Representative photomicrography of lung stained with H&E from an animal in the control group (D), inoculated with the WT (E) or  $\Delta ahpC1$  (F) at 400  $\times$  magnification. Arrows are pointing to neutrophils. C57BL/6 mice were intranasally infected with  $2 \times 10^6$  CFU/mL PA14. Data are expressed as mean  $\pm$  SEM of 8 animals for the infected groups and 3 animals for the control group. Statistical analyses were performed by one-way ANOVA analysis of variance followed by Newman-Keuls. \* $p < 0.05$  indicates a significant difference from control (non-infected) and WT+ABAH groups; # $p < 0.05$  indicates a significant difference from  $\Delta ahpC1$  group.

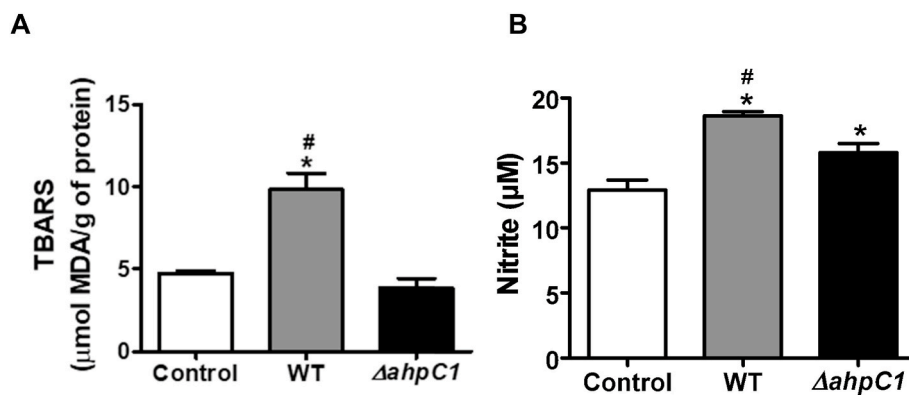


**Fig. 6.** TBARS (thiobarbituric acid-reactive substances) in lung tissue (A) and nitrite in BAL (B) after 24 h of infection. C57BL/6 mice were intranasally infected with  $2 \times 10^6$  CFU/mL wild-type (WT) or  $\Delta ahpC1$  strains. TBARS concentration in the lung was obtained by plotting the absorbance in a malondialdehyde (MDA) standard curve and expressed as  $\mu$ mol of MDA equivalents/g protein. Data are expressed as mean  $\pm$  SEM of 8 animals for the infected groups and 3 animals for the control group. Statistical analyses were performed by one-way ANOVA analysis of variance followed by Newman-Keuls. \* $p < 0.05$  indicates a significant difference from control (non-infected) group # $p < 0.05$  indicates a significant difference from  $\Delta ahpC1$  group.

hyperuricemic mice instilled with sterile saline. Since all infected mice died within three days, we decided to evaluate how this increase in plasma uric acid was affecting cytokine production and release in this initial period of hyperuricemia. The pro-inflammatory cytokines TNF- $\alpha$  and IL-1 $\beta$  were significantly higher in hyperuricemic than normouricemic mice on the 7th day following oxonate injection (Fig. 9C). These results corroborate the above and previous findings [28] by showing that uric acid promotes PA14 survival and infection severity likely by disrupting HOCl production, increasing inflammatory status and tissue damage.  $\Delta ahpC1$  PA14 enhanced virulence in hyperuricemic mice reveals that, despite the fact this strain is more sensitive to the product of uric acid oxidation, urate hydroperoxide, the overall decrease in HOCl and increase in inflammatory status by uric acid are dominant to sustain bacterial virulence *in vivo*.

#### 4. Discussion

The 2-Cys peroxiredoxin AhpC has proven to be an important peroxide detoxifying enzyme [50]. It was described to confer *Francisella tularensis* resistance against superoxide, organic peroxides, H<sub>2</sub>O<sub>2</sub> and nitric oxide donors [66]. In contrast, another study revealed that deletion of AhpC in *Francisella tularensis* did not render a higher susceptibility to H<sub>2</sub>O<sub>2</sub>, only to paraquat (a superoxide generating compound) and to the peroxynitrite generator, SIN-1 [67]. Such difference in H<sub>2</sub>O<sub>2</sub> susceptibility was related to a compensatory effect by catalase that occurs in some *Francisella tularensis* subspecies. Interestingly, the most resistant *Francisella tularensis* SCHU S4 strain was the most sensitive to deletion of AhpC [66,67]. This compensatory effect was also detected in *Helicobacter cinaedi* and *Staphylococcus aureus*, since  $\Delta ahpC$  strain had greater catalase activity [26,27]. An increase in catalase (*kat*) expression occurred by a relief in PerR repression in AhpC mutants [26]. We did not detect this compensatory mechanism in  $\Delta ahpC1$  PA14 since it was much

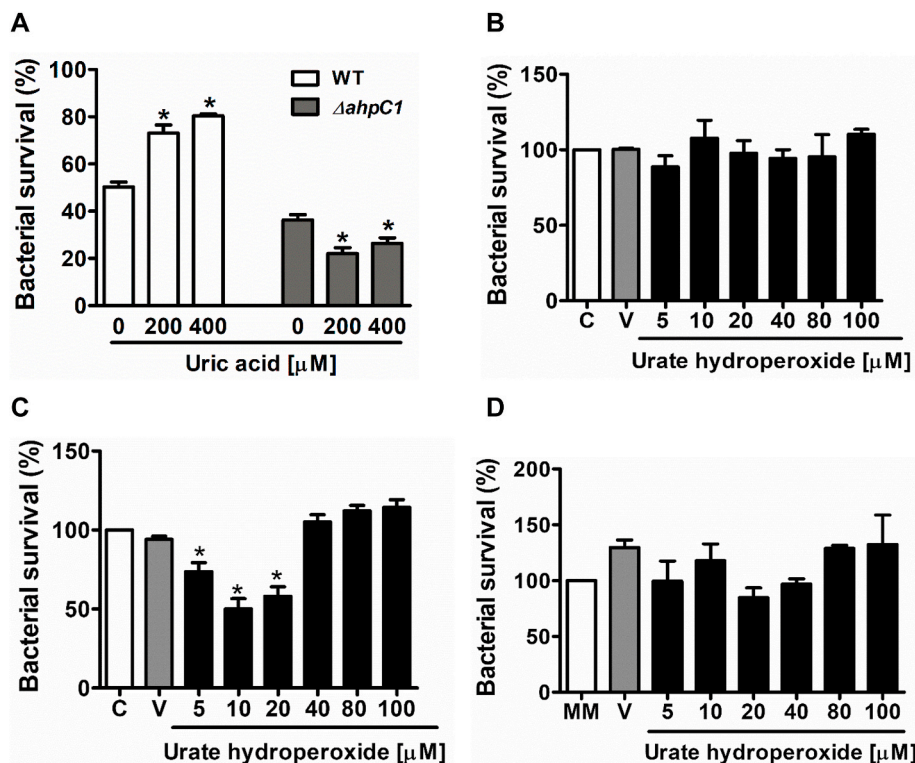


**Fig. 7.** (A) Bacterial survival after incubation with neutrophils in presence or absence of uric acid. Opsonized wild-type or  $\Delta\text{ahpC1}$  ( $1 \times 10^7$  CFU/mL) were incubated with neutrophil ( $1 \times 10^6$  cells/mL) for 1 h in the presence or absence of uric acid. Neutrophils were lysed, samples were diluted 10,000-fold in PBS-glucose. Ten microliters were spread onto MH agar plates and grown for 18–20 h at 30 °C before CFU counting. PA14 survival to urate hydroperoxide in wild-type (B),  $\Delta\text{ahpC1}$  (C) and  $\Delta\text{ahpC1 attB:ahpC1}$  (D). Data were plotted as means  $\pm$  SEM (n = 4). Statistical analyses were performed by one-way ANOVA analysis of variance followed by Newman-Keuls post-test. \*p < 0.05 indicates a significant difference from the group without uric acid in (A) or urate hydroperoxide (B–D). MM: minimal medium; V: urate hydroperoxide vehicle (evaporated mobile phase from HPLC, see methods).

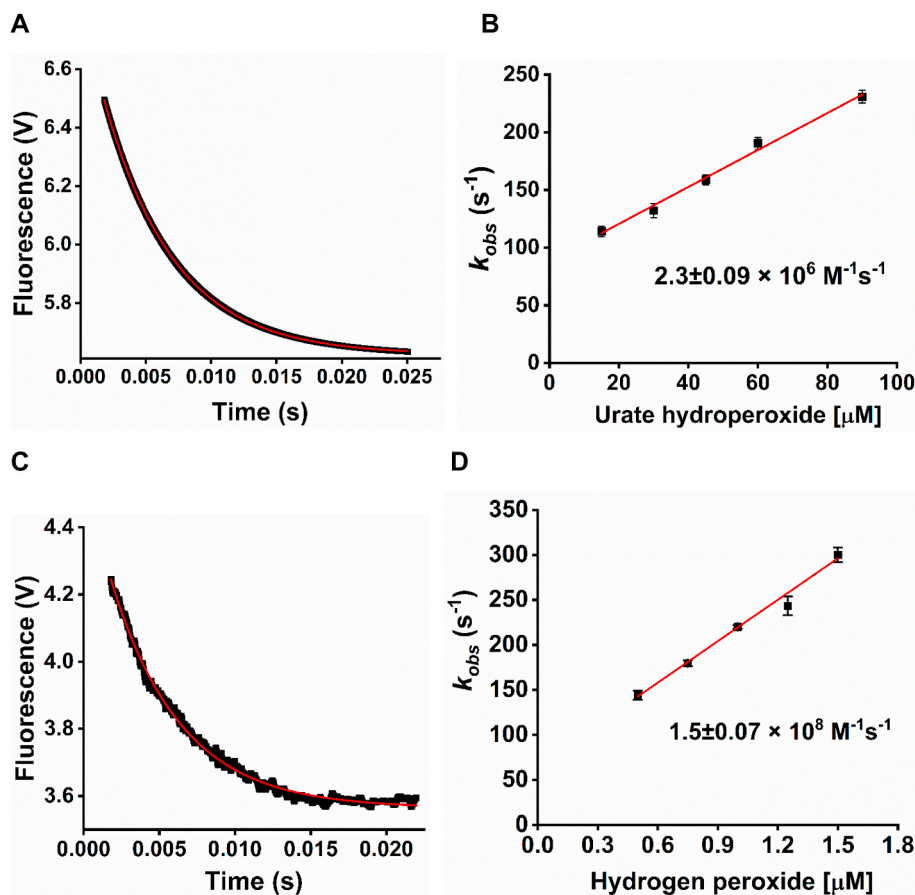


**Fig. 8.** Kinetics for the reduction of urate hydroperoxide (A, B) and hydrogen peroxide (C, D) by AhpC. (A) Pre-reduced AhpC ( $1 \mu\text{M}$ ) was mixed with  $60 \mu\text{M}$  urate hydroperoxide (C) Pre-reduced AhpC ( $0.5 \mu\text{M}$ ) was mixed with  $1 \mu\text{M}$   $\text{H}_2\text{O}_2$  in 50 mM sodium phosphate buffer (pH 7.4, 25 °C) and monitored over time ( $\lambda_{\text{ex}} = 280 \text{ nm}$ ,  $\lambda_{\text{em}} > 340 \text{ nm}$ ) in a stopped-flow device. Data were fitted as a single exponential to obtain the rate constant ( $k_{\text{obs}}$ ) for each peroxide concentration.  $k_{\text{obs}}$  were plotted against varying urate hydroperoxide (B) or  $\text{H}_2\text{O}_2$  (D) concentrations to calculate the second order rate constant from the slope of the linear fitting. V: voltage.

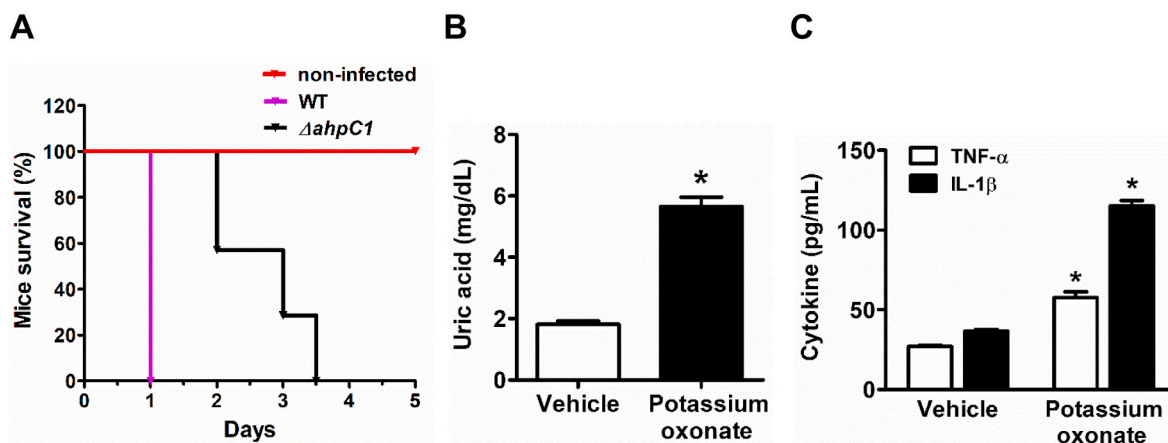


**Fig. 9.** (A) Hyperuricemic C57BL/6 mice survival after intranasal instillation of sterile saline (non-infected), WT or  $\Delta ahpC1$  ( $2 \times 10^6$  CFU/mL). Mice were observed twice a day for survival or any other distress up to 5 days after bacterial instillation. On the 7th day following oxonate treatment, non-infected mice were euthanized for serum uric acid (B) and cytokines (C) measurements. Statistical analyses were performed by one-way ANOVA analysis of variance followed by Newman-Keuls. \* $p < 0.05$  indicates a significant difference from vehicle.

more sensitive to  $H_2O_2$  than the wild-type and the complemented AhpC1. Therefore, despite the antioxidant arsenal present in *Pseudomonas aeruginosa*, no redundancy for AhpC1 was evidenced.

The compensatory mechanism described in those previous studies was detected using very high concentrations of  $H_2O_2$  (0.25–1 M) in the halo assay. Noteworthy, catalase is likely to be much more relevant in such high  $H_2O_2$  concentrations, whereas peroxiredoxins, as AhpC, reduce  $H_2O_2$  at lower, baseline, concentrations [68]. Indeed, AhpC was the primary detoxifier of endogenous  $H_2O_2$  generated by aerobic metabolism, whilst KatE played a major role in scavenging exogenous and supraphysiologic levels of  $H_2O_2$  in *Brucella abortus* [69].

There is a consensus, however, in the protection afforded by AhpC to organic peroxides [26,27,66]. These previous studies revealed a higher sensitivity of  $\Delta ahpC$  strains against *tert*-butyl and cumene hydroperoxide. In the present study we demonstrated, for the first time, the higher sensitivity of an AhpC mutant against a physiological organic peroxide, urate hydroperoxide, which is produced at significant amounts in the inflammatory oxidative burst [30].

We had previously demonstrated that uric acid protected *P. aeruginosa* against the killing activity of neutrophil-like cells. Uric acid is a substrate for myeloperoxidase and dislocates the production of HOCl [28]. Additionally, uric acid can directly scavenge HOCl [70] [–] [72]. The decrease in HOCl was the main cause for the enhanced *P. aeruginosa* survival [28]. If on the one hand uric acid decreased HOCl, on the other hand it increased the oxidative status during the inflammatory oxidative burst. Therefore, the protection afforded by uric acid against bacterial killing was not due to a global antioxidant activity. Urate free radical is the first product from the oxidation of uric acid by myeloperoxidase and it can directly dismutate and hydrate to a more stable product, the hydroxyisourate. In presence of superoxide, as in the inflammatory oxidative burst, the combination of urate free radical with superoxide generates the more stable, but strong oxidant, urate hydroperoxide. Our previous findings suggested that urate hydroperoxide was not as efficient as HOCl to kill *P. aeruginosa* [28]. Here we proved that *P. aeruginosa* is much more sensitive to HOCl ( $IC_{50}$   $19.1 \pm 0.2 \mu M$ ) than to urate hydroperoxide (no killing up to  $100 \mu M$ ) and that this resistance is partially attributed to AhpC1. Noteworthy, deletion of AhpC1 increased the sensitivity to all isolated oxidants: HOCl, urate hydroperoxide and  $H_2O_2$ . AhpC rapidly reduces urate hydroperoxide and  $H_2O_2$ . The rate constants obtained in this study were much similar to that found for the reduction of urate hydroperoxide and  $H_2O_2$  by the human 2-Cys peroxiredoxin Prx2 and the *Salmonella typhimurium* AhpC [49,50,64,65]. We could not calculate the rate constant for the reaction of AhpC with HOCl since the latter also oxidizes tryptophan, interfering

in the intrinsic protein fluorescence. However, the assessment of AhpC dimer formation under incubation with HOCl suggested that this reaction is also very fast (data not shown).

The key role of AhpC1 in urate hydroperoxide detoxification was confirmed by the distinct effect when neutrophils incubated with uric acid were challenged with wild-type or  $\Delta ahpC1$  strains. Whereas uric acid protected wild-type PA14 from neutrophil killing, it increased the killing activity against  $\Delta ahpC1$  PA14. Altogether, these data corroborate the relevance of AhpC1 as a protection mechanism to inflammatory organic peroxides and as a non-redundant factor for *P. aeruginosa* subversion from the innate immune system.

Deletion of AhpC1 highly attenuated *P. aeruginosa* virulence to mice. All survived the 15 days of observation when intranasally infected with  $\Delta ahpC1$ , whereas 100% died before the third day of infection when instilled with wild-type or the complemented  $\Delta ahpC1$  *attB:ahpC1*. Similarly, all mice infected with  $\Delta ahpC$  *Francisella tularensis* survived the 21 days of observation but those infected with wild-type strain died within 8 days of infection [66]. Another study also revealed a prolonged time to death in mice infected with  $\Delta ahpC$  *Francisella tularensis* [73].

Likewise, a much lower number of  $\Delta ahpC1$  *P. aeruginosa* colonized lung and spleen compared to wild-type. As a consequence, a lower number of inflammatory cells was found in bronchoalveolar lavage and lung with lower release of the inflammatory cytokines IL-1 $\beta$  and TNF- $\alpha$  and oxidative stress. Therefore, the absence of AhpC1 in *P. aeruginosa* attenuated the infection capability, shortening bacteria clearance from lung and decreasing tissue inflammation, which increased host survival.

In agreement, deletion of AhpC impaired *Francisella tularensis* replication in bone marrow-derived macrophages and in mice organs [67]. The *Helicobacter cinaedi* *ahpC* mutant was more susceptible to killing by macrophages than the wild-type strain and the cecal colonizing ability of the *ahpC* mutant was significantly reduced in mice [27]. *Mycobacterium tuberculosis* mutant for catalase, which also had less AhpC, had a diminished bacterial growth, lower induction of pro-inflammatory cytokines and significantly reduced pathology scores in infected mice [74]. In contrast, an attenuation in virulence of a double *katA ahpC* mutant was not verified in *Staphylococcus aureus*, but bacterial environmental persistence and nasal colonization were strictly dependent on the presence of these enzymes [26].

*Brucella abortus* *ahpC katE* double mutant had an extremely attenuated virulence and this effect was not attenuated in mice lacking NADPH oxidase or inducible nitric oxide synthase activities, suggesting that host baseline endogenous  $H_2O_2$  production represents a relevant stress to this strain [69]. However, deletion of NADPH oxidase was equally lethal to wild-type and  $\Delta ahpC$  *Francisella tularensis* strains, contrasting the

decreased virulence of *ΔahpC* to wild-type mice [66]. In our hands, inhibition of neutrophils NADPH oxidase or myeloperoxidase significantly increased wild-type and *ΔahpC* PA14 survival in a similar fashion revealing that neutrophil oxidative burst is crucial to PA14 killing despite the presence of AhpC1.

*ΔahpC1* was also less virulent than wild-type PA14 to hyperuricemic mice, contrasting the effect observed in isolated neutrophils, where incubation with uric acid protected wild-type but increased *ΔahpC1* death. Although it seems contrasting, the establishment of hyperuricemia in mice induces a pronounced systemic inflammation [57,75], as confirmed by a significant increase in serum IL-1 $\beta$  and TNF- $\alpha$ . Uric acid is a well-known DAMP (danger-associated molecular pattern) and it primes and/or activates immune cells even in absence of crystals and symptomatic gout [76] [–] [78]. Despite the fact that an immune priming could prepare the immune system to respond faster against pathogens [79], uncontrolled and systemic inflammation can affect organ function and can be related to a worse prognosis in sepsis [80–82]. Although hyperinflammation and sepsis prognosis is a controversial issue [83], an unbalanced inflammatory response and acute renal failure [32,84,85], frequently present in hyperuricemia, is related to a worse prognosis in sepsis [37,83]. In agreement to our experimental data, previous clinical studies have demonstrated that higher levels of serum uric acid are associated with a worse prognosis in sepsis [34] [–] [37]. These clinical studies attributed a worse prognosis to the antioxidant effect of uric acid. Although it may not be the only mechanism, impairment of HOCl production and HOCl neutralization by uric acid is relevant in bacterial survival [28]. Accordingly, oxidation of uric acid is strictly correlated with a worse prognosis in cystic fibrosis by *P. aeruginosa* [33].

In conclusion, this study found that the antioxidant 2-Cys peroxiredoxin AhpC1 is essential for *P. aeruginosa* virulence. AhpC1 efficiently reduced the oxidants H<sub>2</sub>O<sub>2</sub>, urate hydroperoxide and HOCl, which likely contributed to bacterial resistance to the inflammatory oxidative burst. The deletion of the enzyme conferred a much lower virulence to *P. aeruginosa* *in vivo*, as detected through the PA14 intranasal instillation in mice. Peripheral blood neutrophils were more efficient to kill *ΔahpC1* than wild-type and, therefore, bacterial clearance was facilitated in *ΔahpC1* infected mice, decreasing overall inflammatory response and increasing mice survival. In addition, this study demonstrated the key role of this 2-Cys peroxiredoxin in detoxifying organic peroxides, including the novel pro-oxidant urate hydroperoxide, which can be formed in an inflammatory environment in presence of uric acid [30]. Uric acid levels have been associated with an unfavorable prognostic in sepsis [34] [–] [37] and its oxidation was correlated with infection by *P. aeruginosa* in children suffering from cystic fibrosis [33], as well as a higher *P. aeruginosa* survival *in vitro* [28]. Therefore, this study opens up a new insight for the role of antioxidant enzymes in the protection of *P. aeruginosa* and reveals AhpC1 as a promising target to adjuvant antibiotic therapy in persistent infection.

#### Declaration of competing interest

None.

#### Acknowledgments

This work was supported by Fundação de Amparo à Pesquisa do Estado de São Paulo (FAPESP) (CEPID-Redoxoma 2013/07937-8, Young Investigator 2018/14898-2 and multi-user equipment 2015/10411-3 grants), Fundação de Amparo à Pesquisa da Bahia (FAPESB) (RED038/2014) and Conselho Nacional de Desenvolvimento Científico e Tecnológico (CNPq) (462401/2014-6). L.S.R. was a master student from Programa Multicêntrico de Pós-Graduação em Bioquímica e Biologia Molecular (PMBqBM) and received a scholarship from UESB. B.P.S. and R.P.S. received scholarships from FAPESP (2019/26473-9 and 2015/21563-9, respectively). T.M.L.C. received a scholarship from

FAPESB (BOL1270/2017). The authors wish to thank to Prof Dr Amélia Cristina Mendes de Magalhães Gusmão, Prof Dr Lucas Miranda Marques and Prof Dr Regiane Yatsuda from Universidade Federal da Bahia, Instituto Multidisciplinar de Saúde, for providing access to their laboratories for some assays. The authors also thank MSc Lorena L.B. Morbeck for helping in the BAL cell counting, MSc Marcia Aparecida da Silva for technical support in the bacterial survival assay and Prof. Regina Baldini for providing some of the PA14 strains. The graphical abstract was created with BioRender.com.

#### Appendix A. Supplementary data

Supplementary data to this article can be found online at <https://doi.org/10.1016/j.redox.2021.102075>.

#### References

- [1] K. Andersson, N. Carballeira, K.E. Magnusson, C. Persson, O. Stendahl, H. Wolf-Watz, M. Fällman, YopH of *Yersinia pseudotuberculosis* interrupts early phosphotyrosine signalling associated with phagocytosis, *Mol. Microbiol.* 20 (1996) 1057–1069, <https://doi.org/10.1111/j.1365-2958.1996.tb02546.x>.
- [2] S.H.M. Rooijackers, M. Ruyken, A. Roos, M.R. Daha, J.S. Presanis, R.B. Sim, W.J. B. van Wamel, K.P.M. van Kessel, J.A.G. van Strijp, Immune evasion by a staphylococcal complement inhibitor that acts on C3 convertases, *Nat. Immunol.* 6 (2005) 920–927, <https://doi.org/10.1038/ni1235>.
- [3] D. Kraus, A. Peschel, Molecular mechanisms of bacterial resistance to antimicrobial peptides, *Curr. Top. Microbiol. Immunol.* 306 (2006) 231–250, [https://doi.org/10.1007/3-540-29916-5\\_9](https://doi.org/10.1007/3-540-29916-5_9).
- [4] J.T. Buchanan, A.J. Simpson, R.K. Aziz, G.Y. Liu, S.A. Kristian, M. Kotb, J. Feramisco, V. Nizet, DNase expression allows the pathogen group A *Streptococcus* to escape killing in neutrophil extracellular traps, *Curr. Biol.* 16 (2006) 396–400, <https://doi.org/10.1016/j.cub.2005.12.039>.
- [5] Y. Sun, M. Karmakar, P.R. Taylor, A. Rietsch, E. Pearlman, ExoS and ExoT ADP ribosyltransferase activities mediate *Pseudomonas aeruginosa* keratitis by promoting neutrophil apoptosis and bacterial survival, *J. Immunol.* 188 (2012) 1884–1895, <https://doi.org/10.4049/jimmunol.1102148>.
- [6] L. Aussel, W. Zhao, M. Hébrard, A.A. Guilhon, J.P.M. Viala, S. Henri, L. Chasson, J. P. Gorvel, F. Barras, S. Méresse, Salmonella detoxifying enzymes are sufficient to cope with the host oxidative burst, *Mol. Microbiol.* 80 (2011) 628–640, <https://doi.org/10.1111/j.1365-2958.2011.07611.x>.
- [7] J.B. Lyczak, C.L. Cannon, G.B. Pier, Lung infections associated with cystic fibrosis, *Clin. Microbiol. Rev.* 15 (2002) 194–222, <https://doi.org/10.1128/CMR.15.2.194-222.2002>.
- [8] A. Roy-Burman, R.H. Savel, S. Racine, B.L. Swanson, N.S. Revadigar, J. Fujimoto, T. Sawa, D.W. Frank, J.P. Wiener-Kronish, Type III protein secretion is associated with death in lower respiratory and systemic *Pseudomonas aeruginosa* infections, *J. Infect. Dis.* 183 (2001) 1767–1774, <https://doi.org/10.1086/320737>.
- [9] F. Stapleton, N. Carnit, Contact lens-related microbial keratitis: how have epidemiology and genetics helped us with pathogenesis and prophylaxis, *Eye* 26 (2012) 185–193, <https://doi.org/10.1038/eye.2011.288>.
- [10] M. Chatterjee, C.P. Anju, L. Biswas, V. Anil Kumar, C. Gopi Mohan, R. Biswas, Antibiotic resistance in *Pseudomonas aeruginosa* and alternative therapeutic options, *Int. J. Med. Microbiol.* 306 (2016) 48–58, <https://doi.org/10.1016/j.ijmm.2015.11.004>.
- [11] B.J. Berube, S.M. Rangel, A.R. Hauser, *Pseudomonas aeruginosa*: breaking down barriers, *Curr. Genet.* 62 (2016) 109–113, <https://doi.org/10.1007/s00294-015-0522-x>.
- [12] M.H. Diaz, C.M. Shaver, J.D. King, S. Musunuri, J.A. Kazzaz, A.R. Hauser, *Pseudomonas aeruginosa* induces localized immunosuppression during pneumonia, *Infect. Immun.* 76 (2008) 4414–4421, <https://doi.org/10.1128/IAI.00012-08>.
- [13] D. Dacheux, B. Toussaint, M. Richard, G. Brochier, J. Croize, I. Attree, *Pseudomonas aeruginosa* cystic fibrosis isolates induce rapid, type III secretion-dependent, but ExoU-independent, oncosis of macrophages and polymorphonuclear neutrophils, *Infect. Immun.* 68 (2000) 2916–2924, <https://doi.org/10.1128/IAI.68.5.2916-2924.2000>.
- [14] C.M. Shaver, A.R. Hauser, Relative contributions of *Pseudomonas aeruginosa* ExoU, ExoS, and ExoT to virulence in the lung, *Infect. Immun.* 72 (2004) 6969–6977, <https://doi.org/10.1128/IAI.72.12.6969-6977.2004>.
- [15] Y. Apidianakis, L.G. Rahme, *Drosophila melanogaster* as a model host for studying *Pseudomonas aeruginosa* infection, *Nat. Protoc.* 4 (2009) 1285–1294, <https://doi.org/10.1038/nprot.2009.124>.
- [16] J.S. Lee, Y.J. Heo, J.K. Lee, Y.H. Cho, KatA, the major catalase, is critical for osmoprotection and virulence in *Pseudomonas aeruginosa* PA14, *Infect. Immun.* 73 (2005) 4399–4403, <https://doi.org/10.1128/IAI.73.7.4399-4403.2005>.
- [17] G.H. Kaihaji, J.R.F. de Almeida, S.S. dos Santos, L.E.S. Netto, S.R. de Almeida, R. L. Baldini, Involvement of a 1-Cys peroxiredoxin in bacterial virulence, *PLoS Pathog.* 10 (2014) 1004442, <https://doi.org/10.1371/journal.ppat.1004442>.
- [18] S. Atcharpongkul, M. Fuangthong, P. Vattanaviboon, S. Mongkolsuk, Analyses of the regulatory mechanism and physiological roles of *Pseudomonas aeruginosa*

- OhrR, a transcription regulator and a sensor of organic hydroperoxides, *J. Bacteriol.* 192 (2010) 2093–2101, <https://doi.org/10.1128/JB.01510-09>.
- [19] S. Mongkolsuk, W. Praittuan, S. Loprasert, M. Fuangthong, S. Chamnongpol, Identification and characterization of a new organic hydroperoxide resistance (ohr) gene with a novel pattern of oxidative stress regulation from *Xanthomonas campestris* pv. phaseoli, *J. Bacteriol.* 180 (1998) 2636–2643, <https://doi.org/10.1128/jb.180.10.2636-2643.1998>.
- [20] T.G.P. Alegria, D.A. Meireles, J.R.R. Cussiol, M. Hugo, M. Trujillo, M.A. De Oliveira, S. Miyamoto, R.F. Queiroz, N.F. Valadares, R.C. Garratt, R. Radi, P. Di Mascio, O. Augusto, L.E.S. Netto, Ohr plays a central role in bacterial responses against fatty acid hydroperoxides and peroxynitrite, *Proc. Natl. Acad. Sci. U. S. A.* 114 (2017) E132–E141, <https://doi.org/10.1073/pnas.1619659114>.
- [21] N. Somprasong, T. Jittawuttipoka, J. Duang-Nkern, A. Romsang, P. Chaiyen, H. P. Schweizer, P. Vattanaviboon, S. Mongkolsuk, *Pseudomonas aeruginosa* thiol peroxidase protects against hydrogen peroxide toxicity and displays atypical patterns of gene regulation, *J. Bacteriol.* 194 (2012) 3904–3912, <https://doi.org/10.1128/JB.00347-12>.
- [22] U.A. Ochsner, D.J. Hassett, M.L. Vasil, Genetic and physiological characterization of ohr, encoding a protein involved in organic hydroperoxide resistance in *Pseudomonas aeruginosa*, *J. Bacteriol.* 183 (2001) 773–778, <https://doi.org/10.1128/JB.183.2.773-778.2001>.
- [23] J. Lesniak, W.A. Barton, D.B. Nikolov, Structural and functional characterization of the *Pseudomonas* hydroperoxide resistance protein Ohr, *EMBO J.* 21 (2002) 6649–6659, <https://doi.org/10.1093/emboj/cdf670>.
- [24] J.J. LeBlanc, R.J. Davidson, P.S. Hoffman, Compensatory functions of two alkyl hydroperoxide reductases in the oxidative defense system of *Legionella pneumophila*, *J. Bacteriol.* 188 (2006) 6235–6244, <https://doi.org/10.1128/JB.00635-06>.
- [25] Y. Hu, A.R.M. Coates, Acute and persistent *Mycobacterium tuberculosis* infections depend on the thiol peroxidase TPX, *PLoS One* 4 (2009) 5150, <https://doi.org/10.1371/journal.pone.0005150>.
- [26] K. Cosgrove, G. Coutts, I.M. Jonsson, A. Tarkowski, J.F. Kokai-Kun, J.J. Mond, S. J. Foster, Catalase (Kata) and alkyl hydroperoxide reductase (AhpC) have compensatory roles in peroxide stress resistance and are required for survival, persistence, and nasal colonization in *Staphylococcus aureus*, *J. Bacteriol.* 189 (2007) 1025–1035, <https://doi.org/10.1128/JB.01524-06>.
- [27] N. Charoenlap, Z. Shen, M.E. Mcbee, S. Muthupalani, G.N. Wogan, J.G. Fox, D. B. Schauer, Alkyl hydroperoxide reductase is required for helicobacter cinaedi intestinal colonization and survival under oxidative stress in balb/c and balb/c interleukin-10-/- mice, *Infect. Immun.* 80 (2012) 921–928, <https://doi.org/10.1128/IAI.05477-11>.
- [28] L.A.C. Carvalho, J.P.P.B. Lopes, G.H. Kaihami, R.P. Silva, A. Bruni-Cardoso, R. L. Baldini, F.C. Meotti, Uric acid disrupts hypochlorous acid production and the bactericidal activity of HL-60 cells, *Redox Biol.* 16 (2018) 179–188, <https://doi.org/10.1016/j.redox.2018.02.020>.
- [29] R.J. Johnson, E.A. Gaucher, Y.Y. Sautin, G.N. Henderson, A.J. Angerhofer, S. A. Benner, The planetary biology of ascorbate and uric acid and their relationship with the epidemic of obesity and cardiovascular disease, *Med. Hypotheses* 71 (2008) 22–31, <https://doi.org/10.1016/j.mehy.2008.01.017>.
- [30] R.P. Silva, L.A.C. Carvalho, E.S. Patricio, J.P.P. Bonifacio, A.B. Chaves-Filho, S. Miyamoto, F.C. Meotti, Identification of urate hydroperoxide in neutrophils: a novel pro-oxidant generated in inflammatory conditions, *Free Radic. Biol. Med.* 126 (2018) 177–186, <https://doi.org/10.1016/j.freeradbiomed.2018.08.011>.
- [31] M.S. Santana, K.P. Nascimento, P.A. Lotufo, I.M. Benseñor, F.C. Meotti, Allantoin as an independent marker associated with carotid intima-media thickness in subclinical atherosclerosis, Brazilian, *J. Med. Biol. Res.* 51 (2018), <https://doi.org/10.1590/1414-431x20187543>.
- [32] R.J. Johnson, G.L. Bakris, C. Borghi, M.B. Chonchol, D. Feldman, M.A. Lanasa, T. R. Merriman, O.W. Moe, D.B. Mount, L.G. Sanchez Lozada, E. Stahl, D.E. Weiner, G.M. Chertow, Hyperuricemia, acute and chronic kidney disease, hypertension, and cardiovascular disease: report of a scientific workshop organized by the national kidney foundation, *Am. J. Kidney Dis.* 71 (2018) 851–865, <https://doi.org/10.1053/j.ajkd.2017.12.009>.
- [33] N. Dickerhof, R. Turner, I. Khalilova, E. Fantino, P.D. Sly, A.J. Kettle, Oxidized glutathione and uric acid as biomarkers of early cystic fibrosis lung disease, *J. Cyst. Fibros.* 16 (2017) 214–221, <https://doi.org/10.1016/j.jcf.2016.10.012>.
- [34] C.C. Chuang, S.C. Shieh, C.H. Chi, Y.F. Tu, L.I. Hor, C.C. Shieh, M.F. Chen, Serum total antioxidant capacity reflects severity of illness in patients with severe sepsis, *Crit. Care* 10 (2006), <https://doi.org/10.1186/cc4826>.
- [35] K. Tsai, T.G. Hsu, C.W. Kong, K.C. Lin, L.U. Fung-Jou, Is the endogenous peroxyl-radical scavenging capacity of plasma protective in systemic inflammatory disorders in humans? *Free Radic. Biol. Med.* 28 (2000) 926–933, [https://doi.org/10.1016/S0891-5849\(00\)00180-5](https://doi.org/10.1016/S0891-5849(00)00180-5).
- [36] K.L. MacKinnon, Z. Molnar, D. Lowe, I.D. Watson, E. Shearer, Measures of total free radical activity in critically ill patients, *Clin. Biochem.* 32 (1999) 263–268, [https://doi.org/10.1016/S0009-9120\(98\)00109-X](https://doi.org/10.1016/S0009-9120(98)00109-X).
- [37] S.R. Akbar, D.M. Long, K. Hussain, A. Alhajhusain, U.S. Ahmed, H.I. Iqbal, A. W. Ali, R. Leonard, C. Dalton, Hyperuricemia: an early marker for severity of illness in sepsis, *Internet J. Nephrol.* 2015 (2015), <https://doi.org/10.1155/2015/301021>.
- [38] J.C. Toledo, R. Audi, R. Ogusucu, G. Monteiro, L.E.S. Netto, O. Augusto, Horseradish peroxidase compound i as a tool to investigate reactive protein-cysteine residues: from quantification to kinetics, *Free Radic. Biol. Med.* 50 (2011) 1032–1038, <https://doi.org/10.1016/j.freeradbiomed.2011.02.020>.
- [39] M.R. Clausen, K. Huvaere, L.H. Skibsted, J.A.N. Stagsted, Characterization of peroxides formed by riboflavin and light exposure of milk. detection of urate hydroperoxide as a novel oxidation product, *J. Agric. Food Chem.* 58 (2010) 481–487, <https://doi.org/10.1021/jf903470p>.
- [40] E.S. Patricio, F.M. Prado, R.P. Silva, L.A.C. Carvalho, M.V.C. Prates, T. Damos, M. Bertotti, P. Di Mascio, A.J. Kettle, F.C. Meotti, Chemical characterization of urate hydroperoxide, a pro-oxidant intermediate generated by urate oxidation in inflammatory and photoinduced processes, *Chem. Res. Toxicol.* 28 (2015) 1556–1566, <https://doi.org/10.1021/acs.chemrestox.5b00132>.
- [41] L.G. Rahme, E.J. Stevens, S.F. Wolfort, J. Shao, R.G. Tompkins, F.M. Ausubel, Common virulence factors for bacterial pathogenicity in plants and animals, *Science* 268 (80) (1995) 1899–1902, <https://doi.org/10.1126/science.7604262>.
- [42] D.G. Lee, J.M. Urbach, G. Wu, N.T. Liberati, R.L. Feinbaum, S. Miyata, L.T. Diggins, J. He, M. Saucier, E. Déziel, L. Friedman, L. Li, G. Grills, K. Montgomery, R. Kucherlapati, L.G. Rahme, F.M. Ausubel, Genomic analysis reveals that *Pseudomonas aeruginosa* virulence is combinatorial, *Genome Biol.* 7 (2006), <https://doi.org/10.1186/gb-2006-7-10-r90>.
- [43] T.T. Hoang, A.J. Kutchma, A. Becher, H.P. Schweizer, Integration-Proficient Plasmids for *Pseudomonas aeruginosa*: Site-specific Integration and Use for Engineering of Reporter and Expression Strains, 2000, <https://doi.org/10.1006/plas.1999.1441>.
- [44] D. English, B.R. Andersen, Single-step separation of red blood cells, granulocytes and mononuclear leukocytes on discontinuous density gradients of Ficoll-Hypaque, *J. Immunol. Methods* 5 (1974) 249–252, [https://doi.org/10.1016/0022-1759\(74\)90109-4](https://doi.org/10.1016/0022-1759(74)90109-4).
- [45] W. Strober, Trypan blue exclusion test of cell viability, *Curr. Protoc. Immunol.* 3 (2001), <https://doi.org/10.1002/0471142735.ima03bs21>. Appendix.
- [46] C. Vareechon, S.E. Zmina, M. Karmakar, E. Pearlman, A. Rietsch, *Pseudomonas aeruginosa* effector ExoS inhibits ROS production in human neutrophils, *Cell Host Microbe* 21 (2017) 611–618, <https://doi.org/10.1016/j.chom.2017.04.001>, e5.
- [47] B. Horta, M. de Oliveira, K.D.-J. of B., Structural and Biochemical Characterization of Peroxiredoxin Q $\beta$  from *Xylella fastidiosa* Catalytic Mechanism and High Reactivity, *ASBMB*, 2010 (n.d.), <https://www.jbc.org/content/285/21/16051.full.pdf>. (Accessed 14 January 2021).
- [48] A. V. Peskin, F.C. Meotti, L.F. De Souza, R.F. Anderson, C.C. Winterbourn, A. Salvador, Intra-dimer Cooperativity between the Active Site Cysteines during the Oxidation of Peroxiredoxin 2, *BioRxiv* (2020) 2020, <https://doi.org/10.1101/2020.05.11.087908>, 05.11.087908.
- [49] L.A.C. Carvalho, D.R. Truzzi, T.S. Fallani, S.V. Alves, J.C. Toledo, O. Augusto, L.E. S. Netto, F.C. Meotti, Urate hydroperoxide oxidizes human peroxiredoxin 1 and peroxiredoxin 2, *J. Biol. Chem.* 292 (2017) 8705–8715, <https://doi.org/10.1074/jbc.M116.767657>.
- [50] D. Parsonage, K.J. Nelson, G. Ferrer-Sueta, S. Alley, P.A. Karplus, C.M. Furdul, L. B. Poole, Dissecting peroxiredoxin catalysis: separating binding, peroxidation, and resolution for a bacterial AhpC, *Biochemistry* 54 (2015) 1567–1575, <https://doi.org/10.1021/bi501515w>.
- [51] M. Trujillo, A. Clippe, B. Manta, G. Ferrer-Sueta, A. Smeets, J.P. Declercq, B. Knoops, R. Radi, Pre-steady state kinetic characterization of human peroxiredoxin 5: taking advantage of Trp84 fluorescence increase upon oxidation, *Arch. Biochem. Biophys.* 467 (2007) 95–106, <https://doi.org/10.1016/j.abb.2007.08.008>.
- [52] A.V. Peskin, F.M. Low, L.N. Paton, G.J. Maghzal, M.B. Hampton, C.C. Winterbourn, The high reactivity of peroxiredoxin 2 with H<sub>2</sub>O<sub>2</sub> is not reflected in its reaction with other oxidants and thiol reagents, *J. Biol. Chem.* 282 (2007) 11885–11892, <https://doi.org/10.1074/jbc.M700339200>.
- [53] A. Filloux, J.L. Ramos, Preface. *Pseudomonas* methods and protocols, *Methods Mol. Biol.* 1149 (2014), <https://doi.org/10.1007/978-1-4939-0473-0>.
- [54] J.A. Nemzek, H.Y. Xiao, A.E. Minard, G.L. Bolgos, D.G. Remick, Humane endpoints in shock research, *Shock* 21 (2004) 17–25, <https://doi.org/10.1097/01.shk.0000101667.49265.f0>.
- [55] D.A. da Silva, T.M.L. Correia, R. Pereira, R.A.A. da Silva, O. Augusto, R.F. Queiroz, Tempol reduces inflammation and oxidative damage in cigarette smoke-exposed mice by decreasing neutrophil infiltration and activating the Nrf2 pathway, *Chem. Biol. Interact.* 329 (2020), <https://doi.org/10.1016/j.cbi.2020.109210>.
- [56] P. Gueirard, A. Druilhe, M. Pretolani, N. Guiso, Role of adenylate cyclase-hemolysin in alveolar macrophage apoptosis during bordetella pertussis infection in vivo, *Infect. Immun.* 66 (1998) 1718–1725, <https://doi.org/10.1128/iai.66.4.1718-1725.1998>.
- [57] Y. Chen, C. Li, S. Duan, X. Yuan, J. Liang, S. Hou, Curcumin attenuates potassium oxonate-induced hyperuricemia and kidney inflammation in mice, *Biomed. Pharmacother.* 118 (2019) 109195, <https://doi.org/10.1016/j.biopha.2019.109195>.
- [58] L.C. Green, D.A. Wagner, J. Glogowski, P.L. Skipper, J.S. Wishnok, S. R. Tannenbaum, Analysis of nitrate, nitrite, and [15N]nitrate in biological fluids, *Anal. Biochem.* 126 (1982) 131–138, [https://doi.org/10.1016/0003-2697\(82\)90118-X](https://doi.org/10.1016/0003-2697(82)90118-X).
- [59] S.J. Skerrett, C.B. Wilson, H.D. Liggitt, A.M. Hajjar, Redundant Toll-like receptor signaling in the pulmonary host response to *Pseudomonas aeruginosa*, *Am. J. Physiol. Lung Cell Mol. Physiol.* 292 (2007) 312–322, <https://doi.org/10.1152/ajplung.00250.2006>.
- [60] R.F. Queiroz, A.K. Jordão, A.C. Cunha, V.F. Ferreira, M.R.P.L. Brigagão, A. Malvezzi, A.T.D. Amaral, O. Augusto, Nitroxides attenuate carrageenan-induced inflammation in rat paws by reducing neutrophil infiltration and the resulting myeloperoxidase-mediated damage, *Free Radic. Biol. Med.* 53 (2012) 1942–1953, <https://doi.org/10.1016/j.freeradbiomed.2012.09.001>.
- [61] H.H. Draper, E.J. Squires, H. Mahmoodi, J. Wu, S. Agarwal, M. Hadley, A comparative evaluation of thiobarbituric acid methods for the determination of

- malondialdehyde in biological materials, *Free Radic. Biol. Med.* 15 (1993) 353–363, [https://doi.org/10.1016/0891-5849\(93\)90035-5](https://doi.org/10.1016/0891-5849(93)90035-5).
- [62] M.M. Bradford, A rapid and sensitive method for the quantitation of microgram quantities of protein utilizing the principle of protein-dye binding, *Anal. Biochem.* 72 (1976) 248–254, [https://doi.org/10.1016/0003-2697\(76\)90527-3](https://doi.org/10.1016/0003-2697(76)90527-3).
- [63] A.V. Peskin, N. Dickerhof, R.A. Poynton, L.N. Paton, P.E. Pace, M.B. Hampton, C. C. Winterbourn, Hyperoxidation of peroxiredoxins 2 and 3: rate constants for the reactions of the sulfenic acid of the peroxidatic cysteine, *J. Biol. Chem.* 288 (2013) 14170–14177, <https://doi.org/10.1074/jbc.M113.460881>.
- [64] B. Manta, M. Hugo, C. Ortiz, G. Ferrer-Sueta, M. Trujillo, A. Denicola, The peroxidase and peroxynitrite reductase activity of human erythrocyte peroxiredoxin 2, *Arch. Biochem. Biophys.* 484 (2009) 146–154, <https://doi.org/10.1016/j.abb.2008.11.017>.
- [65] A.V. Peskin, F.C. Meotti, L.F. de Souza, R.F. Anderson, C.C. Winterbourn, A. Salvador, Intra-dimer cooperativity between the active site cysteines during the oxidation of peroxiredoxin 2, *Free Radic. Biol. Med.* 158 (2020) 115–125, <https://doi.org/10.1016/j.freeradbiomed.2020.07.007>.
- [66] A. Alharbi, S.M. Rabadi, M. Alqahtani, D. Marghani, M. Worden, Z. Ma, M. Malik, C.S. Bakshi, Role of peroxiredoxin of the AhpC/TSA family in antioxidant defense mechanisms of *Francisella tularensis*, *PloS One* 14 (2019), e0213699, <https://doi.org/10.1371/journal.pone.0213699>.
- [67] J. Binesse, H. Lindgren, L. Lindgren, W. Conlan, A. Sjöstedt, Roles of reactive oxygen species-degrading enzymes of *Francisella tularensis* SCHU S4, *Infect. Immun.* 83 (2015) 2255–2263, <https://doi.org/10.1128/IAI.02488-14>.
- [68] S. Portillo-Ledesma, L.M. Randall, D. Parsonage, J.D. Rizza, P. Andrew Karplus, L. B. Poole, A. Denicola, G. Ferrer-Sueta, Differential kinetics of two-cysteine peroxiredoxin disulfide formation reveal a novel model for peroxide sensing, *Biochemistry* 57 (2018) 3416–3424, <https://doi.org/10.1021/acs.biochem.8b00188>.
- [69] K.H. Steele, J.E. Baumgartner, M.W. Valderas, R.M. Roop, Comparative study of the roles of AhpC and KatE as respiratory antioxidants in *Brucella abortus* 2308, *J. Bacteriol.* 192 (2010) 4912–4922, <https://doi.org/10.1128/JB.00231-10>.
- [70] C.C. Winterbourn, Comparative reactivities of various biological compounds with myeloperoxidase-hydrogen peroxide-chloride, and similarity of oxidant to hypochlorite, *BBA - Gen. Subj.* 840 (1985) 204–210, [https://doi.org/10.1016/0304-4165\(85\)90120-5](https://doi.org/10.1016/0304-4165(85)90120-5).
- [71] G.L. Squadrito, E.M. Postlethwait, S. Matalon, Elucidating mechanisms of chlorine toxicity: reaction kinetics, thermodynamics, and physiological implications, *Am. J. Physiol. Lung Cell Mol. Physiol.* 299 (2010), <https://doi.org/10.1152/ajplung.00077.2010>.
- [72] D. Pattison, M. Davies, Reactions of myeloperoxidase-derived oxidants with biological substrates: gaining chemical insight into human inflammatory diseases, *Curr. Med. Chem.* 13 (2006) 3271–3290, <https://doi.org/10.2174/092986706778773095>.
- [73] K. Kadzhaev, C. Zingmark, I. Golovliov, M. Bolanowski, H. Shen, W. Conlan, A. Sjöstedt, Identification of genes contributing to the virulence of *Francisella tularensis* SCHU S4 in a mouse intradermal infection model, *PloS One* 4 (2009) e5463, <https://doi.org/10.1371/journal.pone.0005463>.
- [74] L.M.R. Nieto, C. Mehaffy, E. Creissen, J.L. Trout, A. Troy, H. Bielefeldt-Ohmman, M. Burgos, A. Izzo, K.M. Dobos, Virulence of *Mycobacterium tuberculosis* after acquisition of Isoniazid resistance: individual nature of katG mutants and the possible role of AhpC, *PloS One* 11 (2016), e0166807, <https://doi.org/10.1371/journal.pone.0166807>.
- [75] W. Baldwin, S. McRae, G. Marek, D. Wymer, V. Pannu, C. Baylis, R.J. Johnson, Y. Y. Sautin, Hyperuricemia as a mediator of the proinflammatory endocrine imbalance in the adipose tissue in a murine model of the metabolic syndrome, *Diabetes* 60 (2011) 1258–1269, <https://doi.org/10.2337/db10-0916>.
- [76] L.A.B. Joosten, M.G. Netea, E. Mylona, M.I. Koenders, R.K.S. Malireddi, M. Oosting, R. Stienstra, F.L. Van De Veerdonk, A.F. Stalenhoef, E.J. Giamarellos-Bourboulis, T.D. Kanneganti, J.W.M. Van Der Meer, Engagement of fatty acids with toll-like receptor 2 drives interleukin-1 $\beta$  production via the ASC/caspase 1 pathway in monosodium urate monohydrate crystal-induced gouty arthritis, *Arthritis Rheum.* 62 (2010) 3237–3248, <https://doi.org/10.1002/art.27667>.
- [77] T.O. Cris an, M.C.P. Cleophas, B. Novakovic, K. Erler, F.L. Van De Veerdonk, H. G. Stunnenberg, M.G. Netea, C.A. Dinarello, L.A.B. Joosten, Uric acid priming in human monocytes is driven by the AKT-PRAS40 autophagy pathway, *Proc. Natl. Acad. Sci. U. S. A.* 114 (2017) 5485–5490, <https://doi.org/10.1073/pnas.1620910114>.
- [78] T.T. Braga, M.F. Forni, M. Correa-Costa, R.N. Ramos, J.A. Barbutto, P. Branco, A. Castoldi, M.I. Hiyane, M.R. Davanzo, E. Latz, B.S. Franklin, A.J. Kowaltowski, N. O.S. Camara, Soluble uric acid activates the NLRP3 inflammasome, *Sci. Rep.* 7 (2017), <https://doi.org/10.1038/srep39884>.
- [79] T.O. Cris an, M.G. Netea, L.A.B. Joosten, Innate immune memory: implications for host responses to damage-associated molecular patterns, *Eur. J. Immunol.* 46 (2016) 817–828, <https://doi.org/10.1002/eji.201545497>.
- [80] L. Thomas, N. Germs, *Engl. J. Med.* 287 (1972) 553–555, <https://doi.org/10.1056/NEJM197209142871109>.
- [81] F. Zeni, B. Freeman, C. Natanson, Anti-inflammatory therapies to treat sepsis and septic shock: a reassessment, *Crit. Care Med.* 25 (1997) 1095–1100, <https://doi.org/10.1097/00003246-199707000-00001>.
- [82] C. Natanson, A.F. Suffredini, P.Q. Eichacker, R.L. Danner, Selected treatment strategies for septic shock based on proposed mechanisms of pathogenesis, in: *Ann. Intern. Med.*, American College of Physicians, 1994, pp. 771–783, <https://doi.org/10.7326/0003-4819-120-9-199405010-00009>.
- [83] R.S. Hotchkiss, I.E. Karl, The pathophysiology and treatment of sepsis, *N. Engl. J. Med.* 348 (2003) 138–150, <https://doi.org/10.1056/nejmra021333>.
- [84] L.G. S anchez-Lozada, V. Soto, E. Tapia, C. Avila-Casado, Y.Y. Sautin, T. Nakagawa, M. Franco, B. Rodr iguez-Iturbe, R.J. Johnson, Role of oxidative stress in the renal abnormalities induced by experimental hyperuricemia, *Am. J. Physiol. Ren. Physiol.* 295 (2008), <https://doi.org/10.1152/ajprenal.00104.2008>.
- [85] P.H.F. Gois, D. Canale, R.A. Volpin, D. Ferreira, M.M. Veras, V. Andrade-Oliveira, N.O.S. C amara, M.H.M. Shimizu, A.C. Seguro, Allopurinol attenuates rhabdomyolysis-associated acute kidney injury: renal and muscular protection, *Free Radic. Biol. Med.* 101 (2016) 176–189, <https://doi.org/10.1016/j.freeradbiomed.2016.10.012>.
- [86] J.C. Morris, The acid ionization constant of HClO from 5 to 35 , *J. Phys. Chem.* 70 (1966) 3798–3805, <https://doi.org/10.1021/j100884a007>.